(NASA-CR-169287) PHOTOVOLTAIC EFFECT IN FERROELECTRIC CERAMICS Final Technical Report, 1 Sep. 1980 - 31 Oct. 1981 (Massachusetts Inst. of Tech.) 62 p HC A04/MF A01 CSCL 11B G3/27

N82-31532

Unclas 32314

SQT

F I N A L T E C H N I C A L R E P O R T

to

NATIONAL AERONAUTICS AND SPACE ADMINISTRATION

by

D. J. Epstein, A. Linz, H. P. Jenssen

Crystal Physics and Optical Electronics Laboratory
Massachusetts Institute of Technology
Cambridge, Massachusetts 02139

entitled

PHOTOVOLTAIC EFFECT IN FERROELECTRIC CERAMICS

April 1982

work performed under

NASA Contract NAG-1-98

September 1, 1980 - October 31, 1981

TABLE OF CONTENTS

I. INTRODUCTION

Ceramic ferroelectrics, when poled, are known to exhibit open-circuit photovoltages that are described as "anomalous" because they can exceed the band-gap voltage of the ferroelectric by many orders of magnitude. The theoretical basis for this effect is not, as yet, on firm ground. The principal model[1] that has been advanced is not particularly quantitative, nor has it been verified under circumstances in which parameter of the model can be obtained in any clean-cut way. The difficulty, of course, is the complexity inherent in the structure and topology of a ceramic material. If photovoltaic studies are done only on ceramics, the prospect for obtaining a reasonably detailed quantitative model is dim.

The object of our program was to try to simulate the ceramic structure in a form that might be more tractable to correlation between experiment and theory. Our approach was based on the use of single crystals (of barium titanate) fabricated in a simple corrugated structure in which the pedestals of the corrugation simulated the grain while the intervening cuts could be filled with materials simulating the grain boundaries. The results of this effort were not successful. The observed photovoltages were extremely small (<100 mv) and our data-taking was plagued by time dependent effects that exhibited considerable variability and made it difficult to establish a defined measurement protocol. Despite this failure, we believe that our approach -- the attempt to simulate a ceramic -- is sound and should be pursued. Variations from our initial

procedures will have to be made, and we point out in this report what these variations might be.

A number of proposals[2,3] have been made for using the anomalous photovoltaic effect in device applications. We caution against any major commitment to device design without there being a better understanding, than now exists, of the basic physical mechanisms responsible for the photo-behavior.

The general theory underlying the ordinary photovoltaic effect is described in Section II. In these theories, the effect is of electrochemical origin, that is, the photogenerated carriers are separated, and then driven, by "built-in" electric fields associated with spatial variations in chemical composition. It is pointed out in Section III that these mechanisms may also account for the anomalous photovoltaic behavior of ceramic ferroelectrics. However, the model proposed in the literature for such materials is of quite a different sort. This model is described and we point out what we believe to be are its shortcomings.

Large photovoltages are also obtained in single crystals and, here, models based upon electrochemical driving forces are no longer applicable. We describe the most appealing model, one in which the driving force for the photocurrent is the preferentially directed release of photoelectrons from anisotropic traps and their preferential recapture. The result is a photocurrent flowing in a direction collinear with the polar axis of the crystal. It is pointed out that this bulk model could account for some of the properties observed in ceramics.

Our experimental work on ceramic $BaTiO_3$ and our efforts to use single crystals of this material to simulate a ceramic, are described in Section IV . Our results on ceramics were in general accord with those reported in the literature. Some of the problems encountered in our attempts to simulate ceramics have already been noted.

A critique of the current state of affairs and our suggestions for further work are contained in Section V.

II. THE PHOTOVOLTAIC EFFECT: GENERAL PROPERTIES

In carrying out a theoretical treatment of the photovoltaic effect, one can direct the analysis either toward finding the short-circuit current or the open-circuit voltage. Examination of the current usually provides more physical insight but, in purely formal sense, the choice is often a matter of convenience only, being dictated by the details of the problem being treated. The two methods will be equivalent provided, always, that appropriate care is taken in defining the photovoltaic circuit. Failure to define the circuit properly can lead to erroneous results.

In Fig. 1 we show a photovoltaic circuit consisting of an inhomogeneously doped semiconductor bar to which contacts A and A' are attached, respectively, at the ends $x = 0$ and $x = L$. A properly defined photovoltaic circuit must satisfy the following conditions. The contacts A and A' must be at the same temperature; they must be made of the same material; and they must be "ohmic". The last condition means that the excess carrier

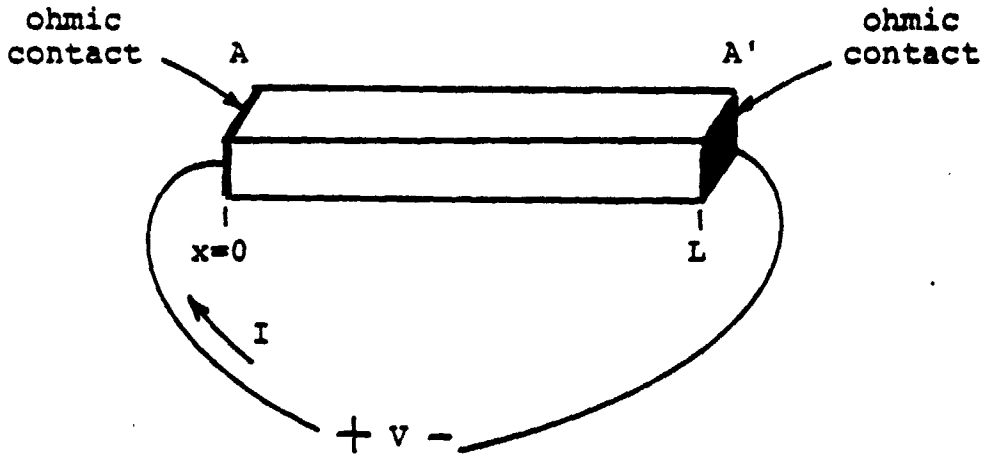

Fig. 1 Photovoltaic circuit.

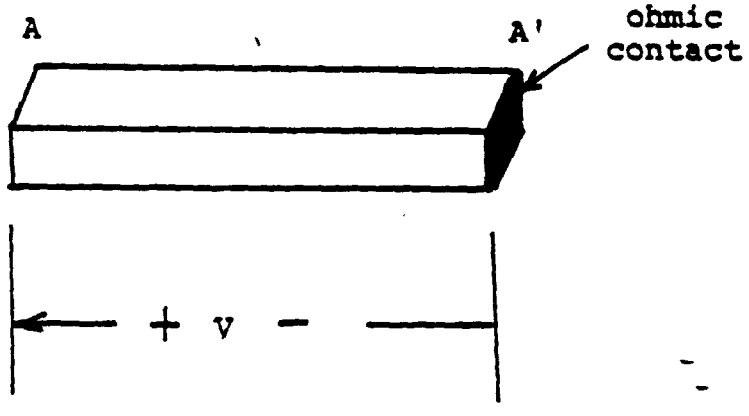

Fig. 2 Improper photovoltaic "circuit".

concentration produced in the bar by illumination must be zero at the surfaces $x = 0^+$ and $x = L^-$. The three conditions taken together guarantee that the contacts A and A' have the same chemical potential and can, therefore, provide the correct reference level for photo-induced potential changes in the circuit.

2.1 Slightly Inhomogeneous Semiconductors

To obtain some insights into the general properties of the photovoltaic effect we shall analyze the circuit in Fig. 1 under the assumption that semiconducting bar is not excessively inhomogeneous. By this statement we mean that changes in dopant concentration or band gap occur only gradually on a distance scale measured in units of the extrinsic Debye length. Under these circumstances we can describe the flow of holes and electrons in the semiconductor by the two equations

$$J_h = q\mu_h pE - qD_h \frac{dp}{dx} \qquad (1)$$

$$J_e = q\mu_e nE + qD_e \frac{dn}{dx} \qquad (2)$$

where J_h = hole current density

μ_h = hole mobility

D_h = hole diffusion coefficient

J_e = electron current density

μ_e = electron mobility

D_e = electron diffusion coefficient

p = hole concentration

n = electron concentration

q = magnitude of the electronic charge

E = electric field

Under conditions of thermodynamic equilibrium the principle of detailed balance requires that the hole and electron currents be separately equal to zero. Thus, from Eq. 1 we have

$$E_o = \frac{D_h}{\mu_h p_o}\left(\frac{dp_o}{dx}\right) \tag{3}$$

where the zero subscripts denote quantities belonging to the equilibrium state. We can rewrite Eq. 3 as

$$E_o = \frac{kT}{q}\ \frac{1}{p_o}\left(\frac{dp_o}{dx}\right) \tag{4}$$

by using Einstein's relation

$$\frac{D}{\mu} = \frac{kT}{q} \tag{5}$$

where k is Boltzmann's constant and T is the absolute temperature. The field E_o is of electrochemical origin, arising because of the sample inhomogeneity described by the term dp_o/dx. We shall refer to E_o as the "built-in field".

In thermodynamic equilibrium, E_o will, of course, not derive a current through the short-circuited bar. To do so would constitute a violation of the second law of thermodynamics. However, E_o will drive any excess carriers produced by optical excitation. We now rewrite Eqs. 1 and 2 for the non-equilibrium case in which excess holes $p' = p-p_o$ and excess electrons $n' = n-n_o$ are optically generated:

$$J_h = q\mu_h\ (p_oE_o + p_oE\ + p'E_o + p'E) - q\ D_h\left(\frac{dp_o}{dx}\ + \frac{dp'}{dx}\right) \tag{6}$$

$$J_e = q\mu_e\ (n_oE_o + n_oE\ + n'E_o + n'E) - q\ D_e\left(\frac{dn_o}{dx} + \frac{dn'}{dx}\right) \tag{7}$$

where we are making the distinction between the build-in field E_o and the applied field E. We know from the requirements imposed by the equilibrium state that the term involving $p_o E_o$ will cancel the one containing dp_o/dx; a similar cancellation will occur for the analogous terms in the equation for J_e. Thus, we obtain

$$J_h = q\mu_h p\, E + q\mu_h p' E_o - qD_h \frac{dp'}{dx} \tag{8}$$

$$J_e = q\mu_e n\, E + q\mu_e n' E_o + qD_e \frac{dn'}{dx} \tag{9}$$

Note that the build-in field E_o drives only the excess concentration while the applied field E drives the total system of carriers. Similarly, the diffusion terms involve only the excess concentrations.

To find the open-circuit photovoltage we impose the requirement that the total current $J = J_h + J_e$ be zero. It follows from Eqs. 8 and 9 that

$$E = - \frac{(\mu_h+\mu_e) p' E_o + (D_h - D_e)(dp'/dx)}{\mu_h p + \mu_e n} \tag{10}$$

where we have assumed quasi-neutrality, i.e. $p' = n'$. If we substitute for E_o from Eq. 4 and use the Einstein relation to replace the terms D_h and D_e by the mobilities μ_h and μ_e we can cast Eq. 10 in the form

$$E = - \frac{kT}{q} \frac{\mu_h + \mu_e}{\mu_h p + \mu_e n} \frac{p'}{p_o} \frac{dp_o}{dx} + \frac{kT}{q} \frac{\mu_h - \mu_e}{\mu_h p + \mu_e n} \frac{dp'}{dx} \tag{11}$$

The open current photovoltage V_{oc} is obtained by integrating the field E to obtain[4]

$$V_{oc} = \int_0^L E dx = V'_{oc} + V''_{oc} \qquad (12)$$

where

$$V'_{oc} = -\frac{kT}{q} \int_0^L \frac{\mu_h + \mu_e}{\mu_h p + \mu_e n} \frac{p'}{p_o} \frac{dp_o}{dx} dx \qquad (13)$$

$$V''_{oc} = \frac{kT}{q} \int_0^L \frac{\mu_h - \mu_e}{\mu_h p + \mu_e n} \frac{dp'}{dx} dx \qquad (14)$$

Note that the term V'_{oc} depends upon both the excess concentration and the spatial variation in p_o, whereas V''_{oc} depends only on the excess concentration. The latter term, which involves the difference in mobility (or diffusion) between holes and electrons, is often referred to as a diffusion potential and is sometimes called the Dember potential.

There is a result of fundamental importance contained in Eq. 12. In a homogeneous material, where $dp_o/dx = 0$, V'_{oc} obviously vanishes. Does V''_{oc} ? The answer depends on the photovoltaic circuit chosen. Suppose the circuit is taken as shown in Fig. 2, where there is an ohmic contact at $x = L$ and a non-ohmic one at $x = 0$. The integration called for by Eq. 14 can be rewritten as

$$V''_{oc} = \frac{kT}{q} \int_0^L \frac{\mu_h - \mu_e}{\mu_h (p_o + p') + \mu_e (n_o + n')} dp' \qquad (15)$$

We note that in the homogeneous sample neither p_o or n_o is a function of x and that because of quasi-neutrality $n' = p'$. It

is clear, therefore, that the integral is a function of p' only, and it follows that

$$V''_{oc} = f(p')\Big|_{x=L} - f(p')\Big|_{x=0} \qquad (16)$$

Thus, it appears that there can be an open-circuit photovoltage between the ends of the bar. However, this voltage cannot drive a current through an external load. To connect to a load, we must introduce an ohmic contact at x = 0 (as in the circuit of Fig. 1). Because p' at x = 0 and x = L are equal (p' = 0 in each case), the value of the function f'(p) at one contact is exactly equal to its value at the other, and, as a result, V''_{oc} vanishes. We conclude that in a homogeneous semiconductor it is impossible to generate a true open-circuit photovoltage via ordinary transport processes. When the sample is inhomogeneous both V'_{oc} and V''_{oc} contribute. The physical mechanism underlying the first term is the built-in potential (arising from the gradient in doping) which separates electrons and holes and provides the e.m.f. for driving them through an external circuit.

2.2 Non-uniform Energy Gap

We shall proceed now to develop a theoretical expression for the open-circuit photovoltage for a semiconductor in which the energy gap varies as a function of position. For ease of calculation we assume the band structure shown in Fig. 3 where the variation in band gap is determined solely by the behavior of the conduction band. The more general problem --- a spatial variation in both bands --- contributes no additional insight into the essential physics of the photovoltaic effect.

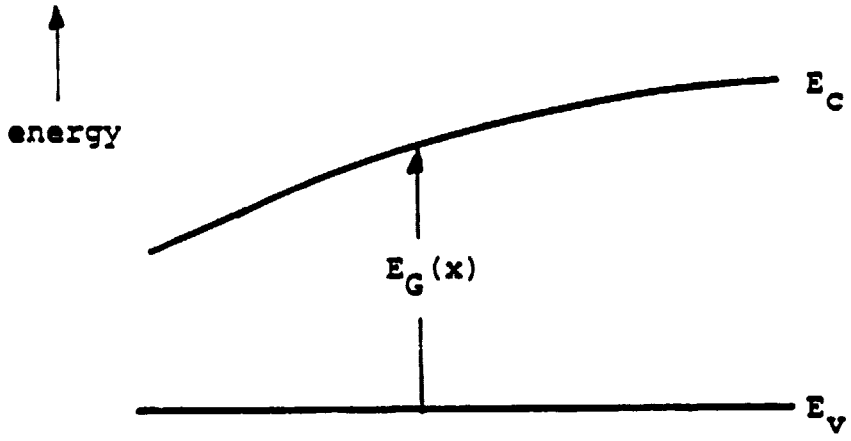

Fig. 3 Semiconductor with spatially varying energy gap $E_G(x)$. E_c is the conduction-band edge, Ev the valence-band edge.

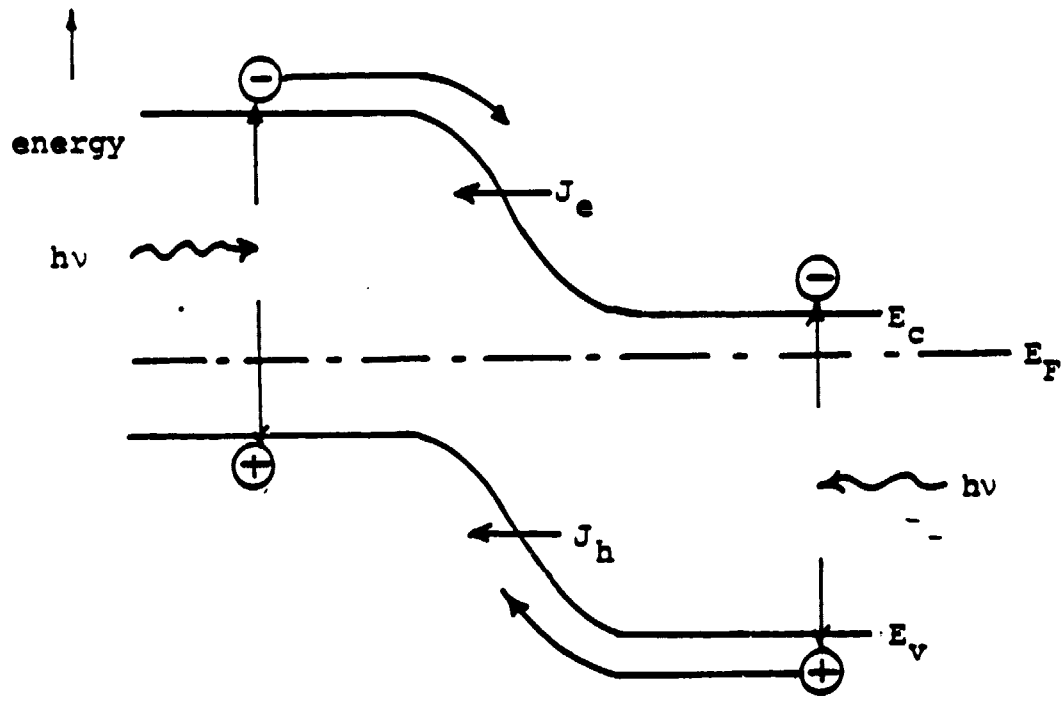

Fig. 4 Photocurrents in illuminated, short-circuited p-n junction. E_F is the Fermi energy.

We proceed as we did in Section 2.1 except we now take into account that the product $n_o p_o$ is a function of position through the variation in the energy gap E_G:

$$n_o p_o = n_i^2 = Ae^{-E_G/kT} \tag{17}$$

The parameter A depends on the density-of-state effective masses of the two bands and these masses, in principle, will depend on x, but we shall make the reasonable assumption that the dependence is weak and that the main variation with x is contained in E_G. It follows that

$$\frac{1}{n_o}\frac{dn_o}{dx} = -\frac{1}{kT}\frac{dE_G}{dx} \tag{18}$$

In the equilibrium state we obtain from Eq. 2 the strength of the built-in field E_{oe}:

$$E_{oe} = \frac{kT}{q}\frac{1}{n_o}\frac{dn_o}{dx} \tag{19}$$

Utilizing Eq. 18, we obtain

$$E_{oe} = -\frac{1}{q}\frac{dE_o}{dx} \tag{20}$$

Because we are assuming $dp_o/dx = 0$ there is no corresponding built-in field for holes.

We return now to Eqs. 2 and 3 to obtain for the hole and electron currents, under illumination

$$J_e = q\mu_e nE + q\mu_e n'E_{oe} + qD_e\frac{dn'}{dx} \tag{21}$$

$$J_h = q\mu_h oE - qD_h\frac{dn'}{dx} \tag{22}$$

where again we have used quasi-neutrality and have recognized that the built-in field will drive only the excess carriers. Using the open circuit condition $J_h + J_e = 0$, we can solve for the E-field in the sample and then integrate this field to obtain the open-circuit potential

$$V_{oc} = \frac{kT}{q} \int_0^L \frac{\mu_h - \mu_e}{(\mu_h p + \mu_e n)} \left(\frac{dn'}{dx}\right) dx$$

$$- \frac{1}{q} \int_0^L \frac{\mu_e}{(\mu_h p + \mu_e n)} \left(n' \frac{dE_G}{dx}\right) dx \qquad (23)$$

The first term is the same as the diffusion potential V''_{oc} described by Eq. 14. The second term is analogous to V'_{oc} as given by Eq. 11, with the energy gap gradient replacing the term $(dp_o/dx)/p_o$ which describes the doping variation in the uniform gap semiconductor.

2.3 Photovoltage in a Junction

When we are dealing with a semiconductor containing a large inhomogeniety, as for example at a junction, we can no longer invoke the quasi-neutrality approximation. To treat the photovoltaic problem, in these circumstances, some form of diode theory is used. The essential physical features of the photodiode are illustrated in Fig. 4. Here we show the band structure for a p-n junction under short circuit conditions. Photons, with energy in excess of the band-gap energy, generate electron-hole pairs in the neutral regions on either side of

the junction. Some of the electrons generated in the p-region diffuse toward the junction, cross the space charge layer and contribute to the majority carrier current on the n-side. The simultaneiously generated holes also diffuse toward the junction, but are turned back by the repulsive junction potential. Thus, the electron-hole pairs generated on the left are separated by the junction potential, and the result is a photocurrent of electrons flowing to the right or a conventional current flowing to the left as a reverse diode current. The carrier pairs generated on the left are also separated by the junction potential which now turns back the electron and passes the holes which provide a second contribution to the reverse current. When an external potential is applied to the photodiode the total current I_D is a superposition of the usual diode current plus the photoinduced reverse current:

$$I_D = I_o[\exp(qV/kT)-1] - I_L \qquad (24)$$

where I_o is the reverse saturation current of the diode and I_L is the photocurrent. The open-circuit voltage is obtained by solving Eq. 24 explicitly for V under the condition $I_D = 0$; thus

$$V_{oc} = \frac{kT}{q} \ln\left[\frac{I_L}{I_o} + 1\right] \qquad (25)$$

The equivalent circuit for the photodiode is shown in Fig. 5.

When a number of individual p-n segments, each with ohmic contacts at its ends, are connected in series, the separate photovoltages add. However, this addition does not occur when the segments are stacked without intervening ohmic contacts.

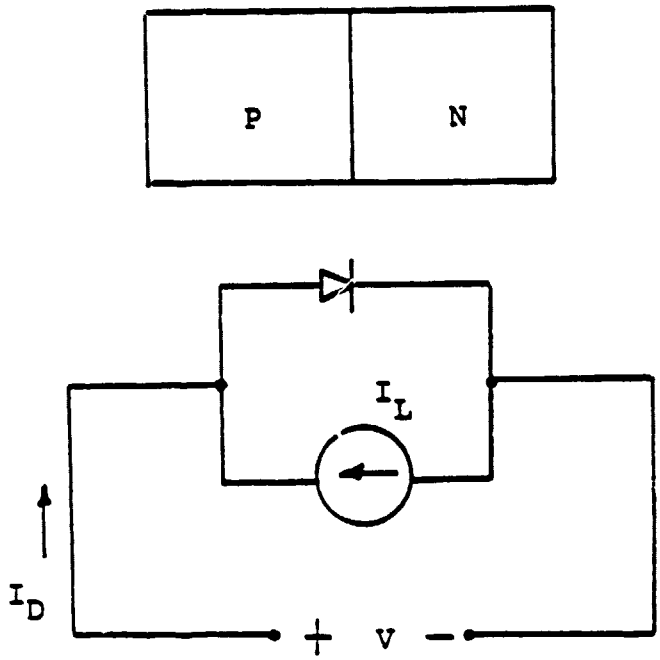

Fig. 5. Equivalent circuit for photodiode.

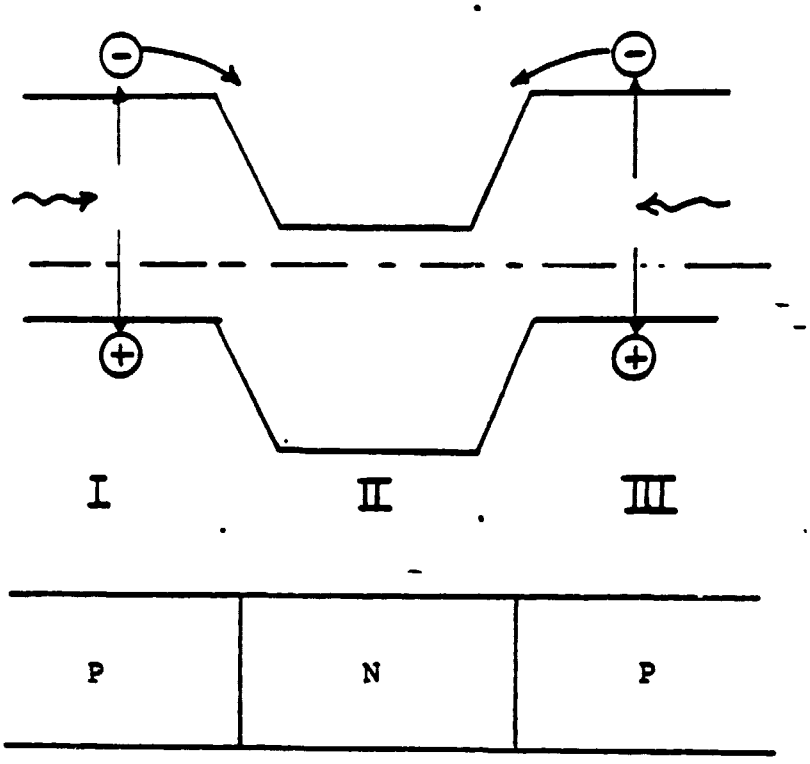

Fig. 6. Cancellation of photocurrents in symmetric p-n-p structure

Consider for example, the symmetric p-n-p configuration shown in Fig.6. Under uniform illumination, electrons generated in region I provide a particle current to the right which is cancelled by an equal and opposite flow of electrons from III to II. Similarly the hole currents cancel. The result is zero photovoltage unless the illumination is nonuniform. If, for example, only the junction I-II were illuminated, there would be a resultant short-circuit photocurrent and, hence, an open-circuit photovoltage.

The problem is easily reduced to circuit terms. The p-n-p structure is topologically equivalent to a transistor and we can therefore employ the Ebers-Moll circuit model suitably modified to include sources of photocurrent (Fig. 7). The diodes in the current represent the behavior of the p-n junctions; the dependent current generations $\alpha_1 I_2$, $\alpha_2 I_1$ account for the electrically injected minority carriers which traverse the n-region without recombining. When the two p-regions are identically doped and geometrically the same, it is readily shown that $\alpha_1 = \alpha_2$, $I_1 = I_2$ and the short circuit current is $I_{L1} - I_{L2}$. It follows that the short-circuit current is identically zero for a uniformly illuminated structure. For there to be a resultant current requires an asymmetric structure and/or non-uniform illumination. The open-circuit voltage can be shown to be given by

$$V_{oc} = \frac{kT}{q} \ln \left(\frac{I_{L1} + \alpha I_{L2}}{I_{L2} + \alpha I_{L1}} \right) \qquad (26)$$

As to be expected this voltage will vanish if $I_{L1} = I_{L2}$.

The circuit representation of Fig. 7 is readily extended to a periodic string of functions (Fig. 8). For M sequential p-n/n-p function pairs -- with every p-region the same, every n-region the same, electrically and geometrically -- the short current will be $I_{L1} - I_{L2}$ as before. The open-circuit voltage will be M times the value V_{oc} given by Eq. 26.

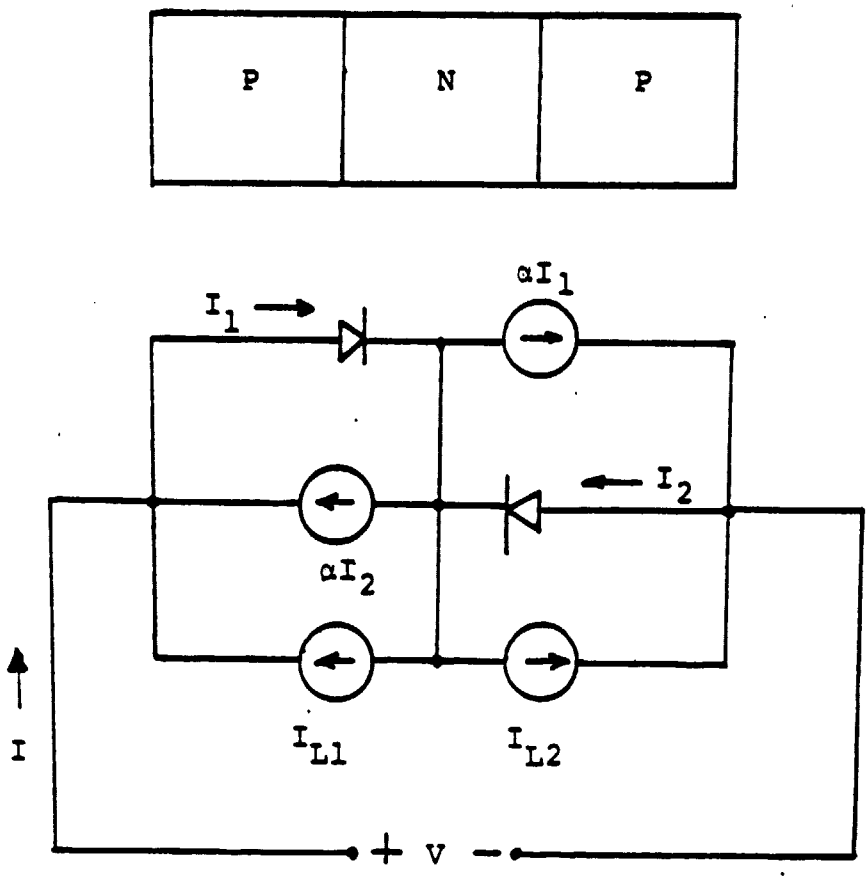

Fig. 7. Ebers-Moll model for illuminated p-n-p structure.

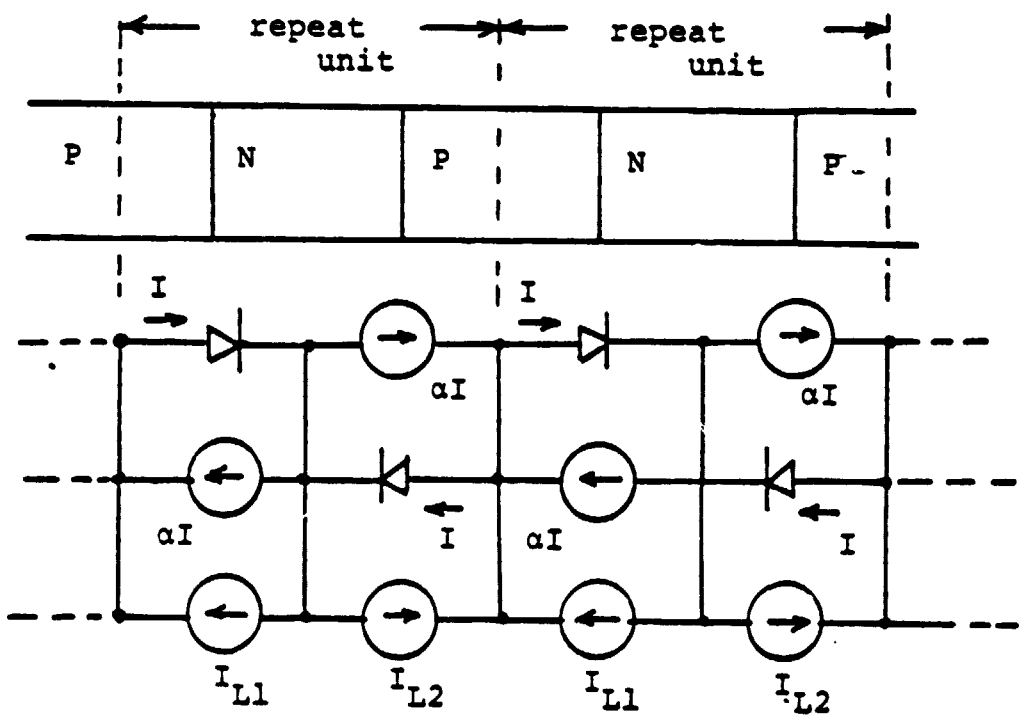

Fig. 8. Circuit model for repeated p-n-p structure.

III. THE PHOTOVOLTAIC EFFECT IN PYROELECTRICS

The special feature that characterizes a pyroelectric is the existence of polar axis in the crystal lattice. The ferroelectrics are a subclass of the pyroelectrics: all ferroelectrics exhibit pyroelectricity, but a pyroelectric need not be ferroelectric.

Most pyroelectrics are relatively good insulators and, consequently, the approach used, in the preceding section, to treat photovoltaic semiconductors cannot be carried over without modification. However, the general physical ideas contained in the preceding discussion remain useful.

In a number of pyroelectrics an anomalously large photovoltage is obtained under open-circuit conditions, the output often ranging up to several thousands of volts. This behavior stands in marked contrast to the behavior in conventional semiconductors where the photovoltage does not exceed the volt equivalence of the energy gap. The theoretical challenge of the anomalous behavior has been met only partly and, even so, more in qualitative than in quantitative terms.

We shall describe two current theories, one due to Brody,[1] the other to Glass.[5,6] The former has been used in an attempt to explain the large photovoltages seen in polarized samples of ceramic ferroelectric. The essential argument here is that each grain develops a small photovoltage (less than band-gap voltage) and that these voltages add, grain-to-grain, to produce a large series sum. It is an experimental fact, however, that very large photovoltages occur in homogeneous single

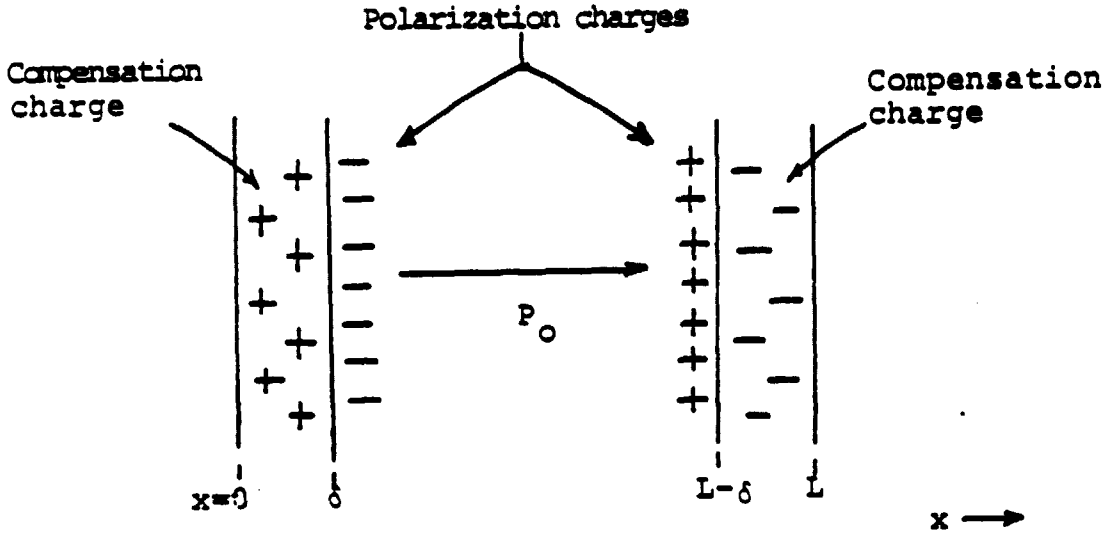

Fig. 9. Model for ferroelectric "grain".

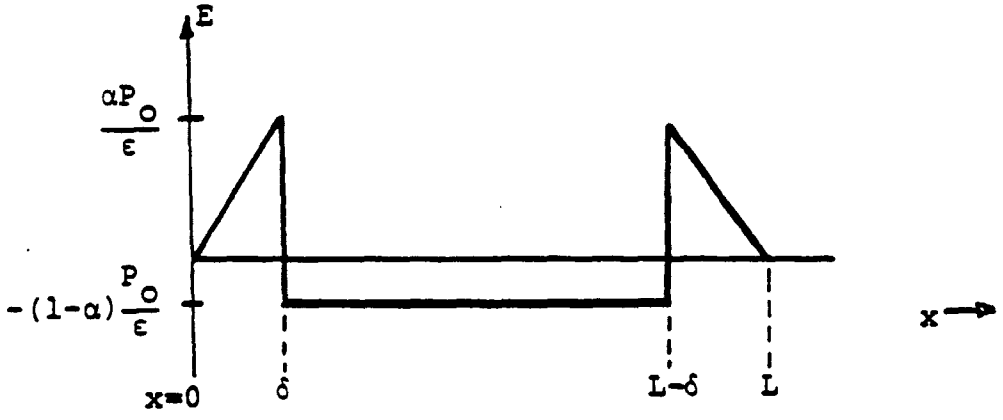

Fig. 10. Electric field distribution in the dark.

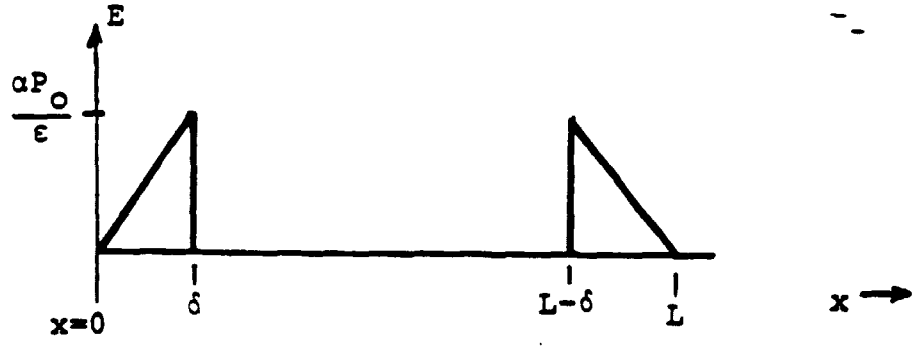

Fig. 11. Electric field in the illuminated "grain".

crystals, a situation where the Brody model clearly cannot apply. To explain the anomalous photovoltages in such cases Glass has proposed a model in which the important feature is the anisotropic recoil of electrons photoexcited from asymmetric traps. This model predicts a continuous photocurrent which, flowing through the highly resistive pyroelectric, is capable of generating a large terminal voltage.

There are, as we shall see, some inherent difficulties with the Brody model, and we shall point out how the main conclusions derived from this model can be arrived at from other points of view.

3.1 Photovoltaic Effect in Ferroelectric Ceramics

To account for the large open-circuit photovoltage observed in ferroelectric ceramics Brody has proposed the following model. The ferroelectric polarization charges within each ceramic grain, in the absence of illumination, are presumed to be neutralized by compensation charges. When the ceramic is illuminated, photogenerated carriers neutralize the polarization charges "exposing" the compensation charges which can then act to produce an electric field in the grain. The integral of the field across the grain gives rise to an elemental photovoltage. When the ceramic is poled, the spontaneous polarization of the collective system of grains tends to align along the poling axis and the elemental photovoltages, similarly aligned, add from grain to grain.

The model for a representative "grain" is shown in Fig. 9. It is assumed that the spontaneous polarization P_o terminates abruptly at the planes $x = \delta$ and $L - \delta$, the resultant

divergence in polarization giving rise to surface charge densities $-P_o$ and $+P_o$ at the respective surfaces. When the ferroelectric is in the dark, these charges are partially neutralized by compensation charges that develop in a "skin" of thickness $\delta << L$. The physical origin of the "skin" is somewhat obscure. There is evidence from work on single crystals that there is a transition region at the surface of a ferroelectric[7], and in a ceramic there is the additional possibility that the "skin" describes the behavior of the grain boundary. The assumption is made, for simplicity, that the compensation charges are distributed uniformly through the thickness δ. We show in an Appendix that the condition of minimum free energy, which must be satisfied for the equilibrium state, requires that the compensation charge have a magnitude αP_o where $\alpha \simeq 1-(\delta/L)$. The resultant electric field distribution is shown in Fig. 10. Note that inside the bulk of the "grain", $\sigma < x < L-\delta$, there exists a negatively directed E-field.

Brody now assumes that, when the grain is illuminated, the electron-hole pairs generated within the grain's bulk move, under the influence of the residual E-field to the ends of the grain and, by doing so, cancel the E-field in the bulk. The resultant field distribution, shown in Fig. 11, differs from zero only in the skin regions. The photovoltage per grain, obtained by integrating this field from $x = L$ to 0, is

$$V = \frac{\alpha P_o \delta}{\epsilon} \qquad (27)$$

The point x = 0 is the positive end of the grain and therefore, the sign of the photovoltage has the same polarity as the voltage used in establishing the spontaneous polarization. This feature of the model is in agreement with what is found experimentally. The model is also consistent with the experimental finding that the value of the photovoltage tends to follow the magnitude of the spontaneous polarization, and that the voltage tends to be inversely related to the grain size.

While the theory is successful in accounting for a major body of experimental fact, it is largely qualitative and is by no means unique. Moreover, it suffers from a serious flaw which can be made evident by a reexamination of Fig. 10. The field distribution shown has been derived on the assumption that the ferroelectric is a perfect insulator. However, any real material will have a finite conductivity and will not be able to sustain an electric field for an indefinite time. The field must eventually disappear with a time constant given by the dielectric-relaxation time σ/ε. Thus, the assumption of a non-vanishing E-field as an equilibrium property of the unilluminated ferroelectric is not valid. It is possible to have "built-in" fields in an equilibrium situation, but these are electrochemical in origin, i.e. they arise as a result of inhomogeneities in composition, as, for example, in an inhomogeneously doped semiconductor. In Brody's model the fields are of electromagnetic origin and as such they must vanish in the presence of finite conductivity.

3.2 Photovoltaic Effect in Single Crystals

The discovery of large photovoltages in ceramics was antedated by observations of similar anomalous behavior in pyroelectric crystals. The phenomenon was first seen in certain samples of ZnS, ostensibly single crystal, which, on closer examination, turned out to have alternating striations of cubic and hexagonal phases. Explanation for the photoeffect in this system[8,9] have been pursued within the framework of the kind of semiconductor transport theory we have discussed in Sec. II. The resulting models no doubt incorporate the important qualitative features of the semiconductor physics, but are weak on quantitative details.

The anomalous photovoltaic voltages seen in certain ferroelectric oxides (e.g. $LiNbO_3$, $BaTiO_3$) cannot be explained in terms of conventional transport theory. It appears that in these cases we are dealing with a bulk effect that occurs without there being any need for internal junctions or any other form of sample inhomogeneity. The only reasonable model that has thus far been advanced is one due to Glass et al.[5] In this model the photoeffect is attributed to the photoexcitation of electrons trapped in anisotropic potential wells. The mechanism is illustrated in Fig. 12. In the dark, the trapped electron is in the ground state E_o of an anisotropic potential well. When light of sufficient energy is applied, the electron is raised to a state of energy $V_1<E<V_2$. The electron is free to move to right but is restricted in its motion to the left by the shoulder of the asymmetric barrier. The existence of a

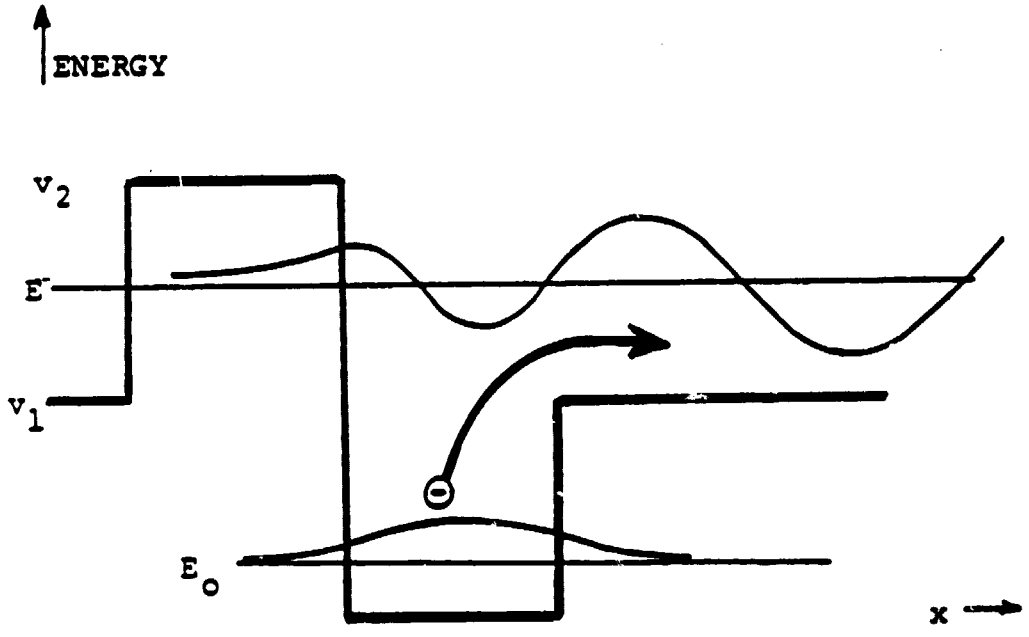

Fig. 12. Electron photoexcited from anistropic trap. The ground state and excited state wave functions are shown.

polar axis in the crystal implies that the asymmetry of the potential well will maintain the same sense throughout the crystal and, consequently, the statistical ensemble of photo-excited electrons will show a preferred direction of excitation into the conduction band. The result will be a directed excitation current of the form

$$J_{ph,exc} = \frac{q\alpha\Phi}{h\nu}\left[p'_+ \lambda_+ - p_- \lambda_- + Z_i \Delta X_i\right] \tag{28a}$$

Here Φ is the light intensity, α the absorption coefficient, p_+ and p_- are, respectively, the probability for electron transfer in the positive and negative polarization directions, and λ_+ and λ_- are the corresponding mean free paths for charge transfer in two directions. The term $Z_i \Delta X_i$ accounts for the current produced by the displacement ΔX_i of the ionized impurity (of charge qZ) that remains after the photoelectron has been excited. The net photocurrent must be calculated by taking the difference between the excitation current and the recombination current that arises when the excited electrons are retrapped. The net current is

$$J_{ph} = \frac{q\alpha\Phi}{h\nu}\left[p_+\lambda_+ - p_-\lambda_- + p'_+\lambda'_+ - p'_-\lambda'_- + Z_i\Delta Z_i - Z'_i\Delta X'_i\right] \tag{28b}$$

The primed quantities are all parameters of the recombination process. If we apply an external potential to the photoconductor, thereby establishing an electric field E inside the ferroelectric, the resultant current is

$$J = J_{ph} + \sigma E \tag{29}$$

where σ is the electrical conductivity of the illuminated sample. The open-circuit voltage is readily found by setting $J = 0$ and integrating the resultant field over the length of the sample L:

$$V_{oc} = -EL = + \frac{J_{ph}L}{\sigma} \qquad (30)$$

Thus, even though the photoeffect may be small, in the sense that it might give rise to a very small short-circuit photocurrent, the open-circuit voltage can be large, provided the sample conductivity is low.

3.3 Remarks on the Photovoltaic Effect in Ceramic Ferroelectrics

Having expressed disfavor with the theory proposed by Brody what have we to offer by way of alternatives. Our belief is that any satisfactory theory will have to include: (1) intrinsic bulk effects of the kind found in homogeneous single crystals; (2) junction effects occurring at the grain-grain boundary.

The difficulty, at this time, in considering alternatives is that given the limited experimental information now available there are just too many alternatives. The theory proposed by Glass, et al. quite readily accounts for a number of the important experimental results found in ceramic ferroelectrics. The relation between the magnitude of the photovoltage and the state of polarization is easily explained: aligning the polarization from grain to grain assures that the photocurrents in adjacent grains will add along a common polar axis. The observation that the photovoltage increases in proportion to

the number of grains/cm might simply indicate that we are dealing with a bulk photocurrent, as proposed by Glass, flowing through a sample whose resistance is determined to a large extent by the number of grain boundaries encountered by the current. The more grain boundaries/cm the higher the resistance and, according to Eq. 30, the higher the photovoltage.

Explanations for the anomalous effect in ceramics may well be contained in the semiconductor models considered in Sec. II. Consider, for example, the open-circuit photovoltage arising from the second term in Eq. 23:

$$V_{oc,G} = -\frac{1}{q}\int_0^L \frac{\mu_e}{(\mu_e p+\mu_h n)}\, n'\, \frac{dE_G}{dx}\, dx \qquad (31)$$

The important quantities here are n', the excess carrier concentration produced by illumination, and the term dE_G/dx describing the spatial variation of the energy gap. If we assume that the excess carriers n', p' are small compared to n and p we can rewrite Eq. 31 in the form

$$V_{oc,G} = -\frac{\mu_e}{\sigma}\int_0^L n'\, \frac{dE_G}{dx}\, dx \qquad (32)$$

where we have recognized that the conductivity σ is given by $q(\mu_e p+\mu_h n)$. Assume now that the photoexcited carrier density n'(x) is nonuniform. If we expand the spatial variation in a Fourier series and, for simplicity, focus our attention on the fundamental component

$$n'(x) = n_o \cos(2\pi x/a) \quad , \qquad (33)$$

the fundamental spatial period "a" can be identified with the grain size of the ceramic. Similarly, we can expand the energy gap variation $E_G(x)$ in a Fourier series, and, again, looking only at the fundamental, we have

$$E_G(x) = E_{Go} \sin [(2\pi x/a) + \theta] \tag{34}$$

It follows that

$$n' \frac{dE_G}{dx} = \eta_o E_{Go} \frac{\pi}{a} [\cos(4\pi \frac{x}{a} + \theta) + \cos \theta] \tag{35}$$

When this is integrated over L, which is presumed to be equal to an integral multiple of the grain size "a", we obtain

$$V_{oc,G} = - \frac{\pi \mu_e \eta_o E_{G_o}}{\sigma} (L/a) \cos \theta \tag{36}$$

We note that this result is compatible with two experimental features of the photovoltaic effect in ferroelectric ceramics: the direct proportionality between photovoltage and sample length, and the inverse dependence on the grain size. We see, however, that the phase factor is extremely important. If θ were a random variable that averaged out to zero, there would be no photovoltage. However, we can make the plausible argument that existence of ferroelectric polarization can lead to a favorable value for θ. In Fig. 13 we show, in schamatic form, a band structure in an interval "a" which spans a "grain/grain-boundary" interval. The gap is presumed to be largest at the "grain" center and to decrease gradually as the region of the "grain boundary" is entered. Such an assumption reflects the fact that the grain

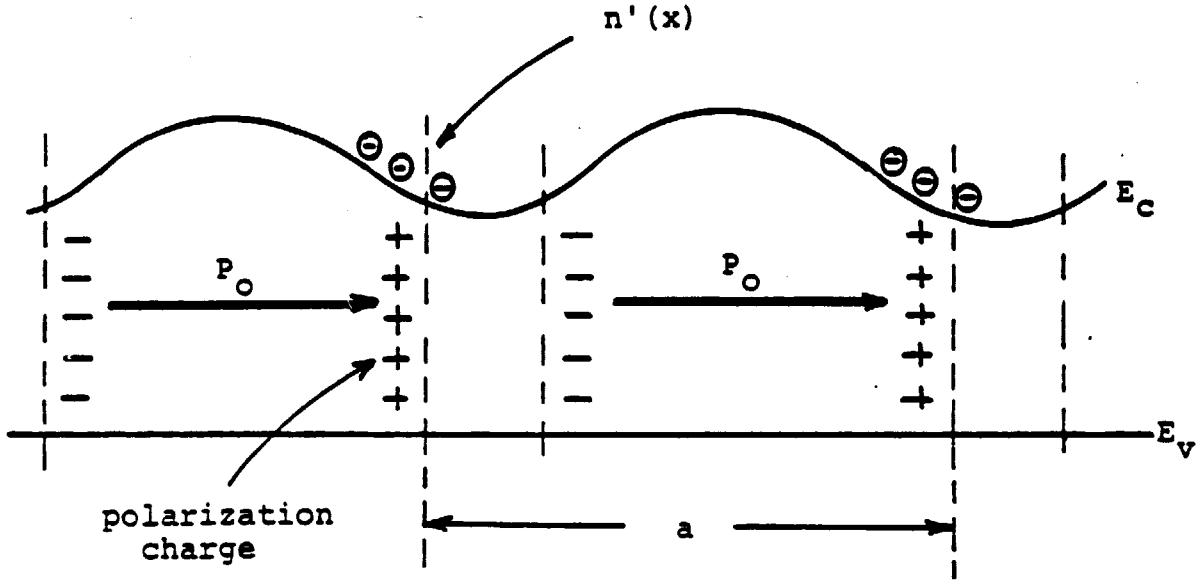

Fig. 13. The fundamental Fourier components of n'(x) and dE_G/dx are out of phase; cos θ = -1.

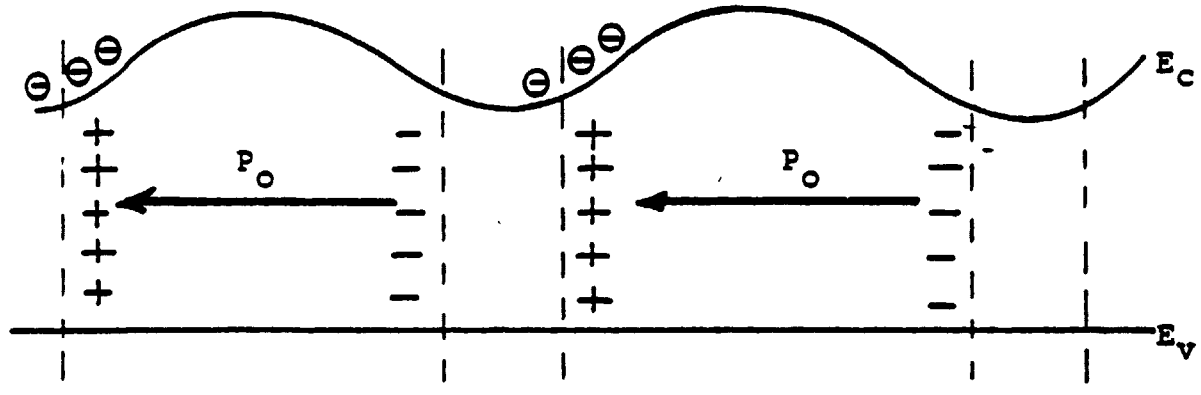

Fig. 14. The fundamental Fourier components of n'(x) and dE_G/dx are in phase; cos θ = +1.

boundary regions contain a larger number of defects and these can cause band-states to tail off into the gap, thereby causing an effective reduction in the gap. We also assume that because of these defects and because of voids between grains, the spontaneous polarization is discontinuous from grain-to-grain. The resultant polarization charges, produced by this discontinuity, are now able to influence the steady state distribution of photoexcited electrons: the electron concentration n' will tend to cluster at the positive polarization charges as shown in Fig. 13. The resultant Fourier components of $n'(x)$ and dE_G/dx are out of phase, i.e. $\cos\theta = -1$. Thus, we have a photovoltage

$$V_{oc,G} = \frac{\pi \mu_e \eta_o E_{Go}}{\sigma} \left(\frac{L}{a}\right) \qquad (37)$$

The polarity of the voltage is in the same sense as the applied voltage used in polarizing the ferroelectric in the +x direction and is the one experimentally observed. When the polarization is established in the -x direction the photoelectrons cluster as shown in Fig. 14, $\cos\theta$ becomes +1, and the sign of the photovoltage changes as it should.

Although this model is successful in "explaining" the experimental facts we make no claim to its "correctness". The point we wish to emphasize is, that given the present state of our knowledge about the anomalous photovoltage, it is possible to cook up a variety of models, all of which may be plausible, but none of which may be "true". Much more in the way of exerimental work is needed before confidence can be given to any proposed model. We shall return to this point in the final section of this report.

IV. EXPERIMENTAL PROGRAM

In order to establish a connection with previous work, we began our investigation with measurements on ceramic ferroelectrics. We then proceeded to study the photovoltaic behavior of a single crystal machined in a geometry that was intended to provide a controlled simulation of a ceramic morphology.

4.1 Ceramic Ferroelectrics

4.1.1. Sample Preparation

Samples, in the shape of rectangular parallelipeds, were cut, with a diamond saw, from a ceramic disc of barium titanate, $BaTiO_3$. Sample lengths varied from 1.54 cm to 0.7 cm; all samples were 0.57 cm wide and 0.1 cm thick. Contacts were applied to the ends of each sample by evaporating, first, a 100 A° thick Cr Film, followed by a gold evaporation of the same thickness. Insulated wire leads were bonded to the contacts with a conductive silver epoxy paste which was cured at 150°C.

Each sample was suspended by its leads in a quartz optical cell which was clamped in an aluminum holder that was then mounted on an optical bench.

The samples were poled by applying DC fields in the range 5 - 20 KV/cm. Fields greater than 22KV/cm exceeded the breakdown strength of the ceramic.

4.1.2. Measurements

Open-circuit photovoltage and short-circuit photocurrent, measured as a function of light intensity, are shown

in Fig. 15. The data were obtained on a sample 1.54 cm long polarized to a remanent state 3.5 μcoul/cm^2 and illuminated by 390 nm radiation. The illumination source was a Xenon arc lamp whose output was passed through a Bausch and Lomb monochromator. Light-intensity measurements were made with a Molectron PR-100 pyroelectric radiometer.

The open-circuit photovoltage was measured with a Keithley 602 electrometer (input impedance>10^{14} ohms) and the short-circuit current was measured with the same electrometer connected in its current measurement mode. The photocurrent is a linear function of light intensity; the photovoltage, in contrast, is strongly nonlinear, exhibiting saturation as the light intensity is increased.

The photovoltage, when measured under fixed conditions of light intensity, wavelength, and polarization, shows a linear variation with sample length (Fig. 16).

Measurements of sample resistance as a function of light intensity are shown in Fig. 17. The behavior suggests that the photocarrier production depends on the light intensity in a nonlinear way.

The dependence of photovoltage and photocurrent on remanent polarization is shown in Fig. 18. The data shows considerable scatter but the trends are essentially linear for both quantities.

The wavelength dependence of the photocurrent (Fig. 19) is strongly peaked in the vicinity of the absorption edge (~390 nm). The photovoltage behaves in a markedly different way, being almost

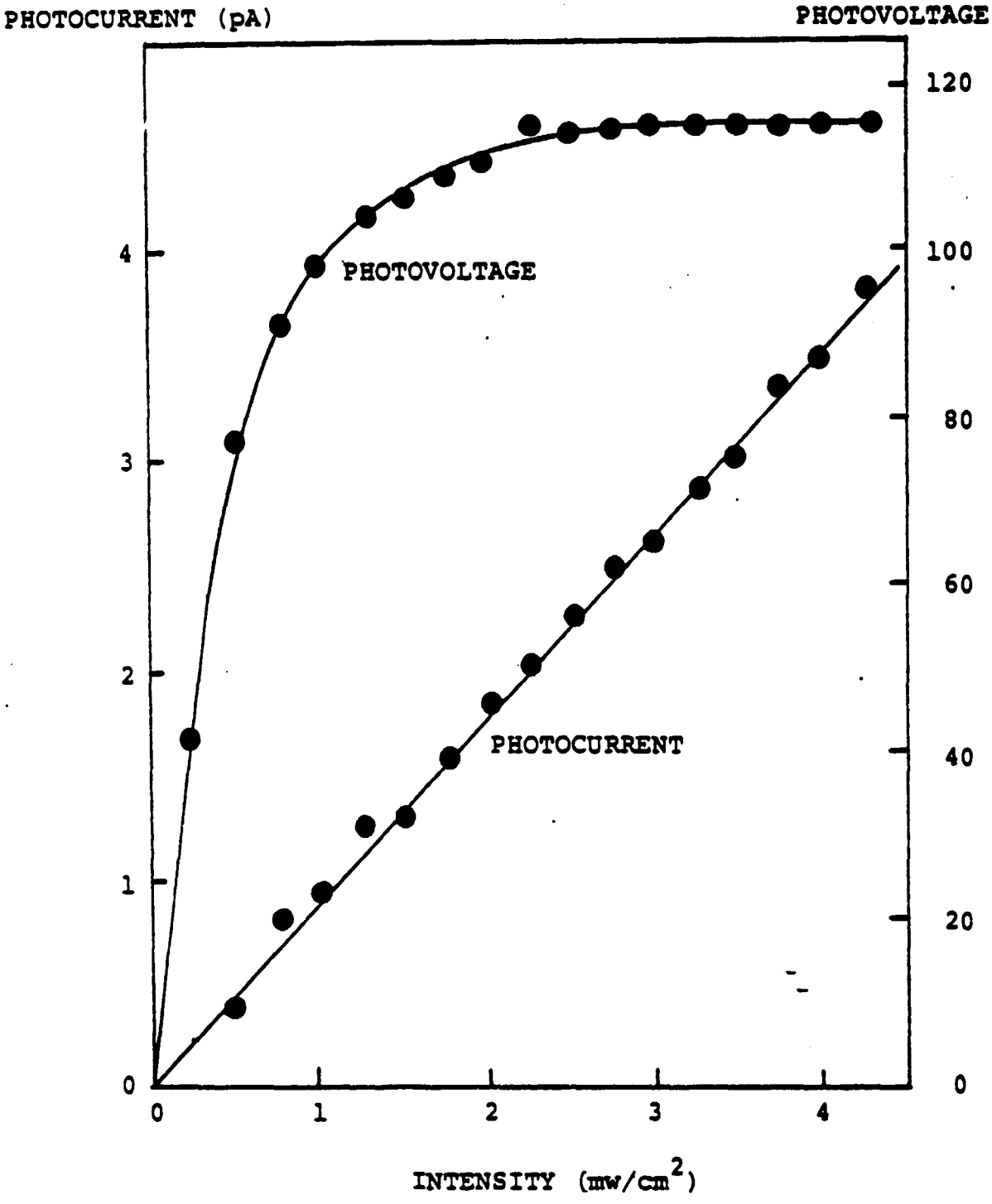

Fig. 15. Open-circuit photovoltage and short-circuit photocurrent as a function of light intensity. Sample lenth 1.54 cm; wavelength 390 nm; remanent polarization 3.5 μC/cm^2.

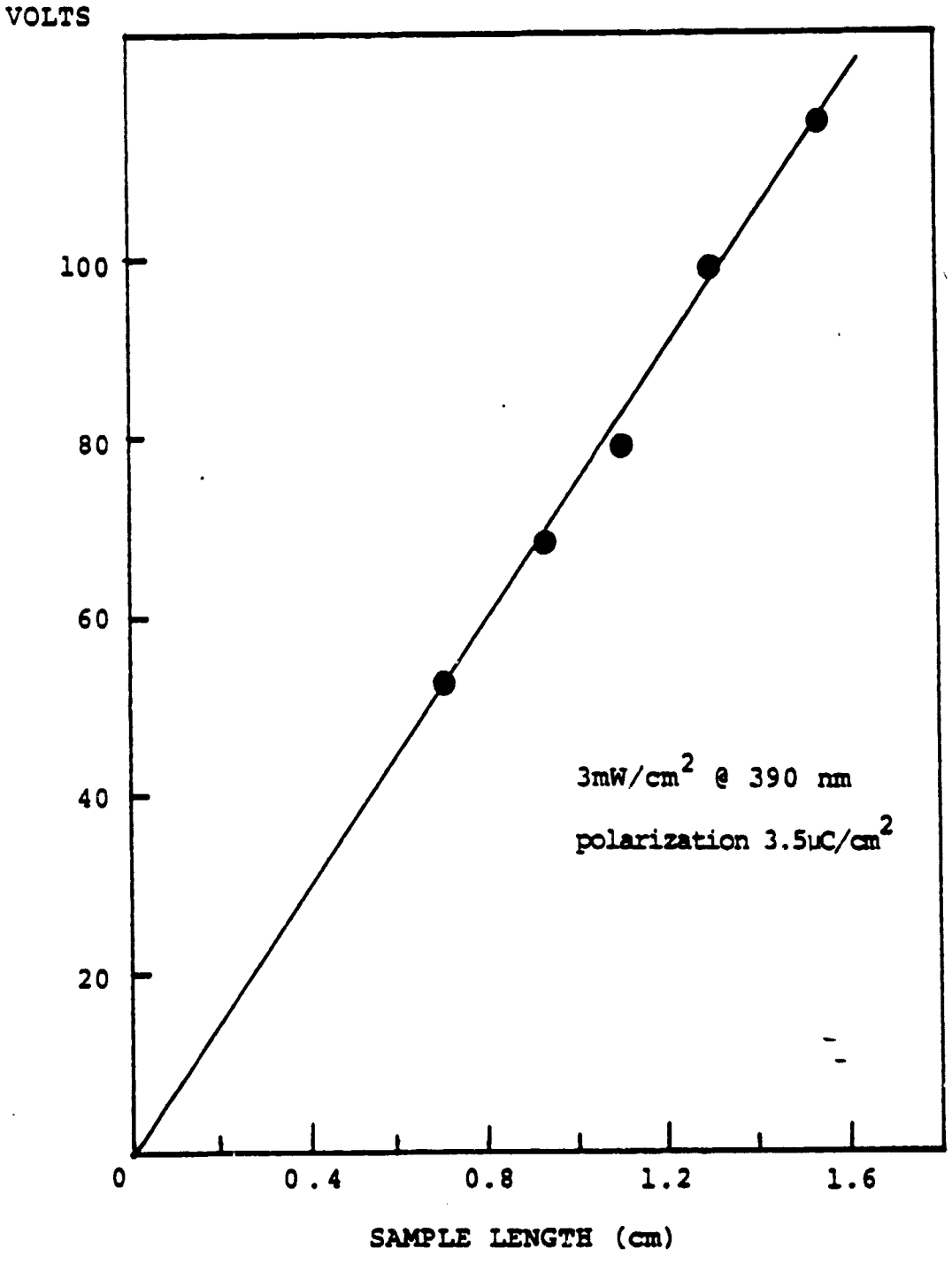

Fig. 16. Open-circuit photovoltage as a function of sample length.

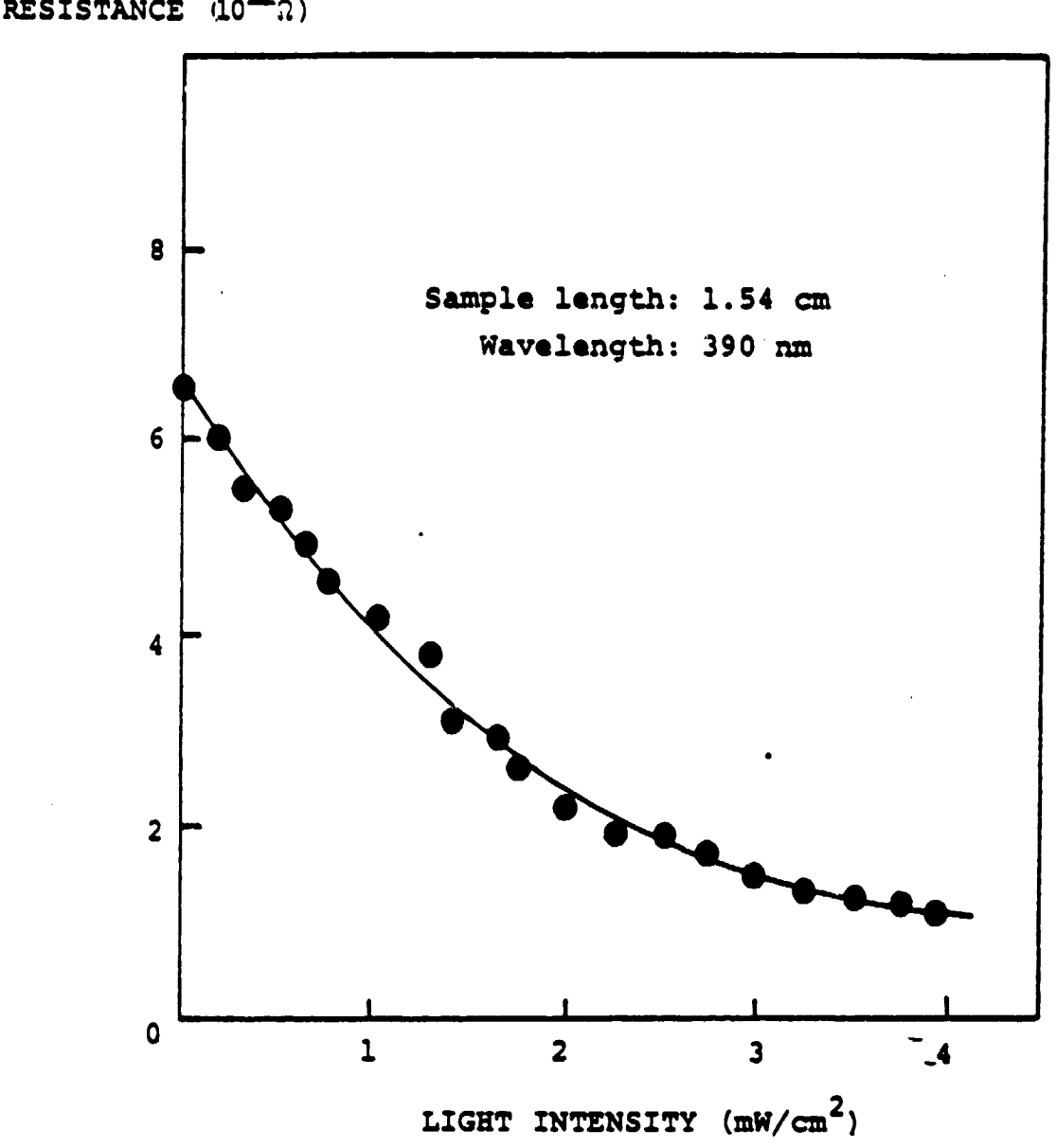

Fig. 17. Resistance as a function of light intensity.

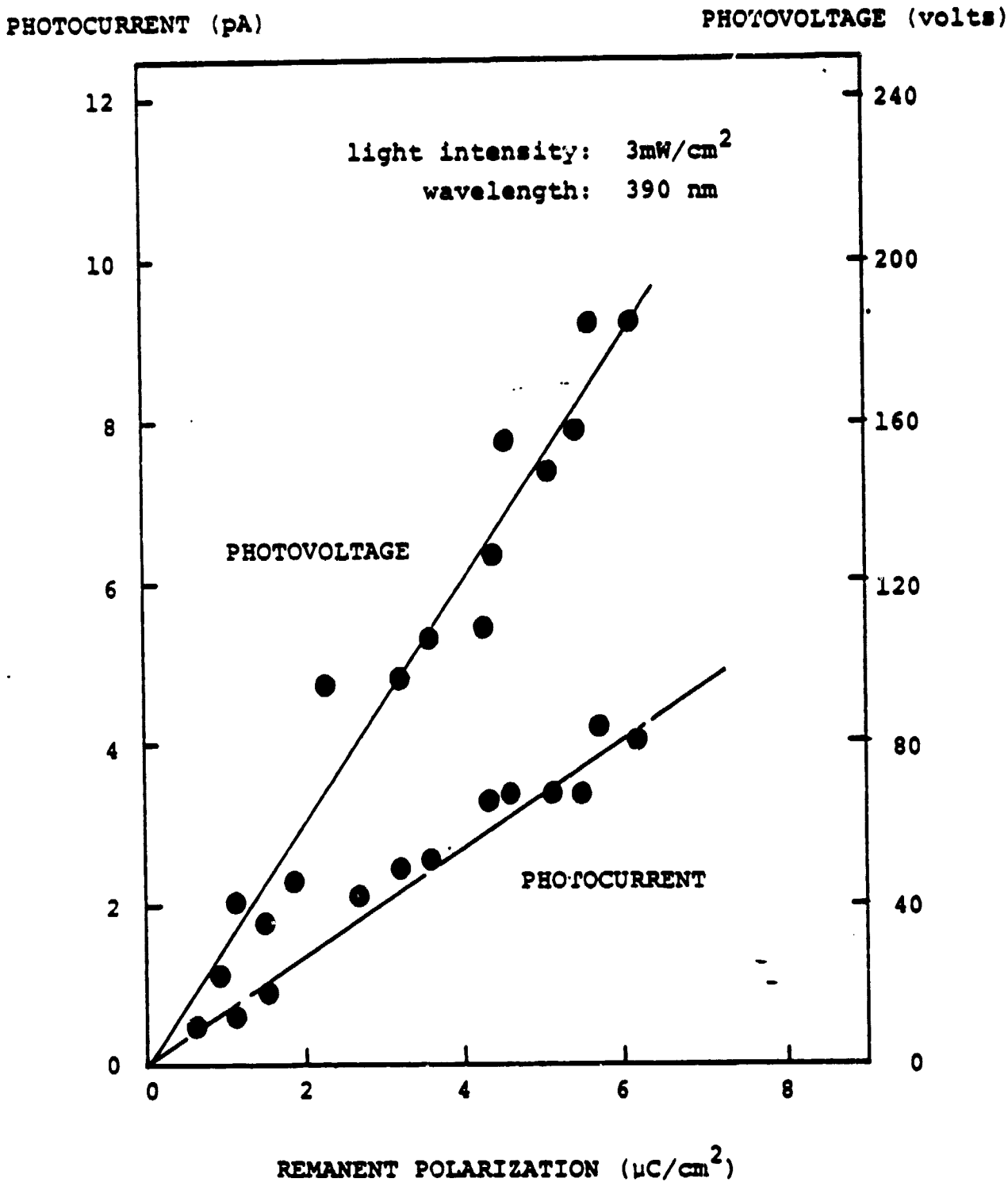

Fig. 18. Photocurrent and photovoltage as a function of remanent polarization.

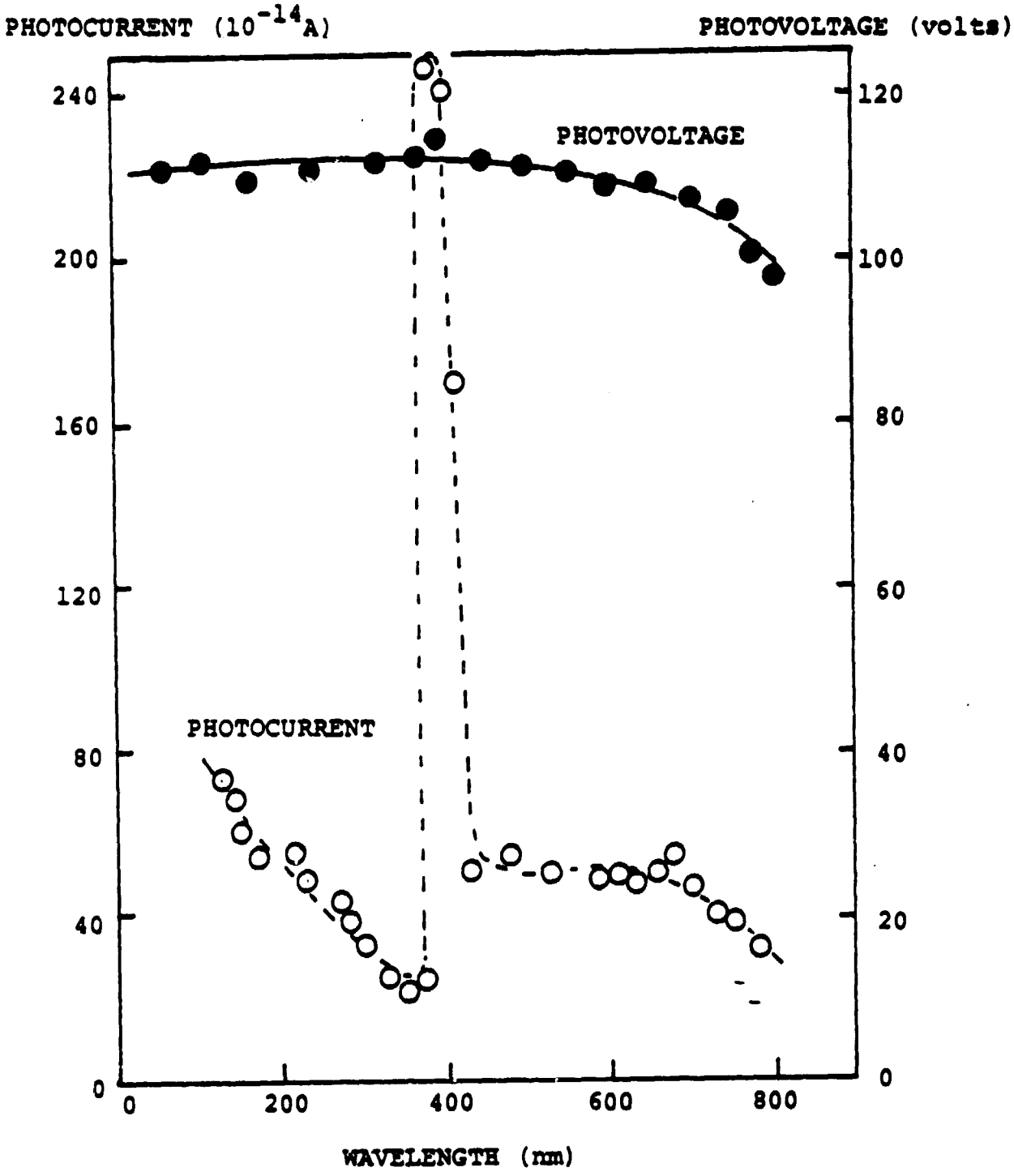

Fig. 19. Wavelength dependence of photocurrent and photovoltage. The light intensity was 3 mW/cm^2; remanent polarization was 3.5 μC/cm^2.

independent of wavelength out to between 100-800 nm with only a slight fall off at the longer wavelengths.

The experimental results we have obtained are in general agreement with what has been reported in the literature.

There are a number of features in the data which appear satisfyingly simple. The linear variation of photovoltage with sample length and with remanent polarization is quite plausible. The linear variation of short-circuit photocurrent with light intensity implies that the photogenerated carrier concentration must also be a linear function of the light intensity, but why then does the photoresistance show no such linear behavior. Clearly, we are not dealing with transport processes that are simple. The short circuit photocurrent has a pronounced maximum as a function of wavelength, but the photovoltage shows no such anomaly. Are we to regard the photovoltage as a more fundamental quantity than the photocurrent or vice versa. The answer to this question has important implications for the development of a satisfactory theory. In Brody's model the photovoltage is the basic quantity. In Glass' model and in the transport models we have discussed the photocurrent is the more fundamental quantity.

4,2 Single Crystal Measurements

The ceramic ferroelectric is far too complex a structure to enable the performance of controlled experiments that might lead to a reasonably quantitative theory of the anomalous photovoltaic effect. We sought, therefore, to create a simpler structure that might exhibit some of the features of the ceramic:

(1) a series of "grains" in which the polarization axis could be easily defined; (2) "grain boundaries" containing a material of composition different from the "grain". The configuration we chose, shown in Fig. 20, involves a single domain crystal of $BaTiO_3$ into which surface corrugations were cut. The pedestals in the structure form the "grains". The grain boundaries" are obtained by filling the cuts with various materials.

4.2.1. Preparation of the Single Crystal

For our single crystal studies we chose to work with barium titanate for two main reasons. The ferroelectric properties of the material have been very well characterized and high quality single crystals, grown by the top-seeded solution method, were available from previous research carried out in our Laboratory.

From a bulk single crystal we cut five bars, each approximately 2 x 3 x 9 mm, oriented with the long axis parallel to a [100] crystallographic direction. The dark resistance of these bars were extremely high, $> 10^{13}$ ohm, making it difficult to do reliable electrical measurements. We, therefore, reduced one of the bars in H_2 at 600°C for 8 hours. The resistance dropped to $5 \times 10^9 \Omega$ and the sample showed a measureable UV photoconductive response.

It was not possible to pole the sample at room temperature by applying voltages up to 8kV. Some poling could be achieved mechanically by squeezing the side faces of the sample between glass discs, but a single domain could not be obtained. To improve the domain structure it was necessary to heat the sample

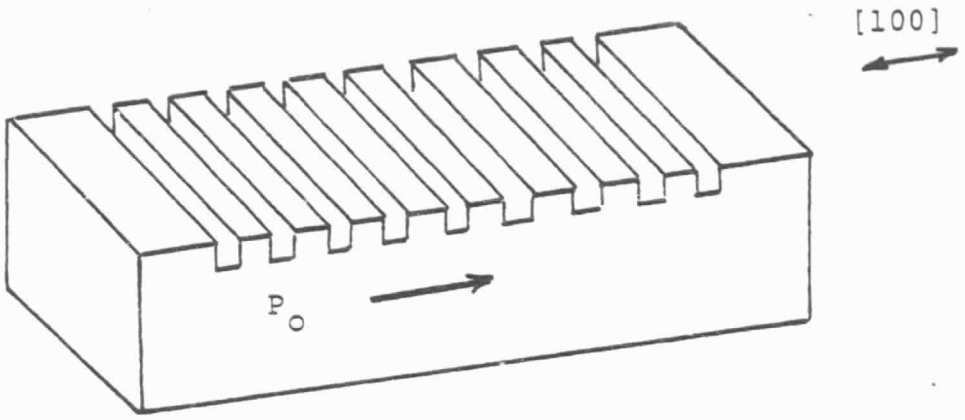

Fig. 20. Corrugated crystal.

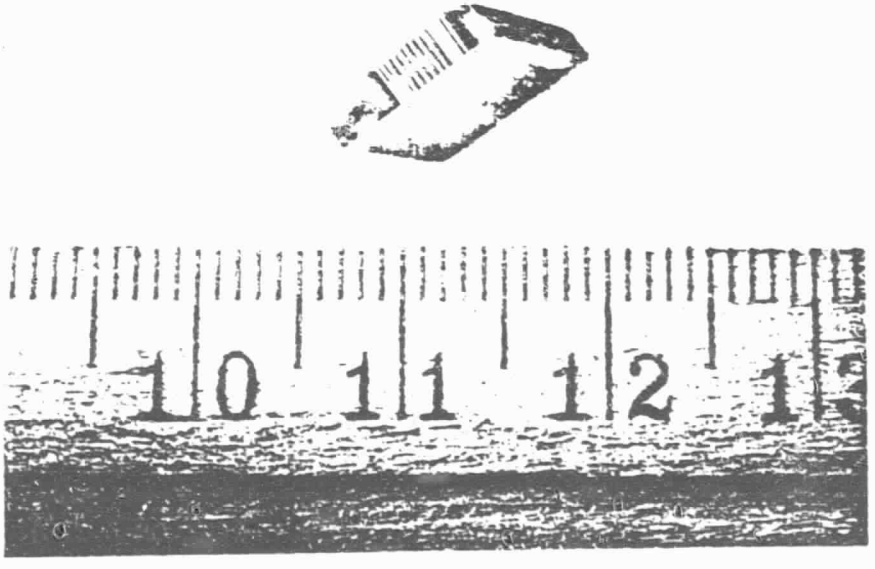

Fig. 21. Corrugated single crystal of barium titanate, $BaTiO_3$.

in mineral oil to 140°C (5°C above the Curie point) and then slowly cool it with 3.5 kV applied across the length of the bar. Examined between crossed polarizers, the treated bar proved to be essentially single domain, showing only a few residual domain walls.

Thirteen grooves approximately 1mm deep and spaced 10-15 mils apart were cut into one of the 3 x 9 mm faces of the bar with a 5 mil string saw. The resultant crystal is shown in Fig. 21. Visible domain structure was affected only slightly by the cutting operation.

4.2.2. Measurements

In our measurements of photovoltage the sample was illuminated by a 75W Xenon source, filtered with a CS-7-54 filter that only allowed passage of radiation shorter than 400 nm. Because the sample absorption edge is ∿400 nm (Fig. 22) the radiation we used was absorbed primarily at the surface and therefore, our photovoltaic measurements represent the behavior of the corrugated region and not the bulk of the crystal.

In our initial experiments the "grain boundaries" were formed by evaporating gold on the sample and then removing the gold from all surfaces, except those in the grooves, by careful mechanical polishing. To our surprise the resistance of the sample dropped to 4 x $10^7\Omega$. By reoxidizing at 600°C the resistance was brought up to $>10^{12}$ ohm. Photovoltages obtained with gold in the "grain boundaries" were extremely small and, consequently, we next explored silver paste as a filler material. The photovoltages, although larger than for gold, remained small and the

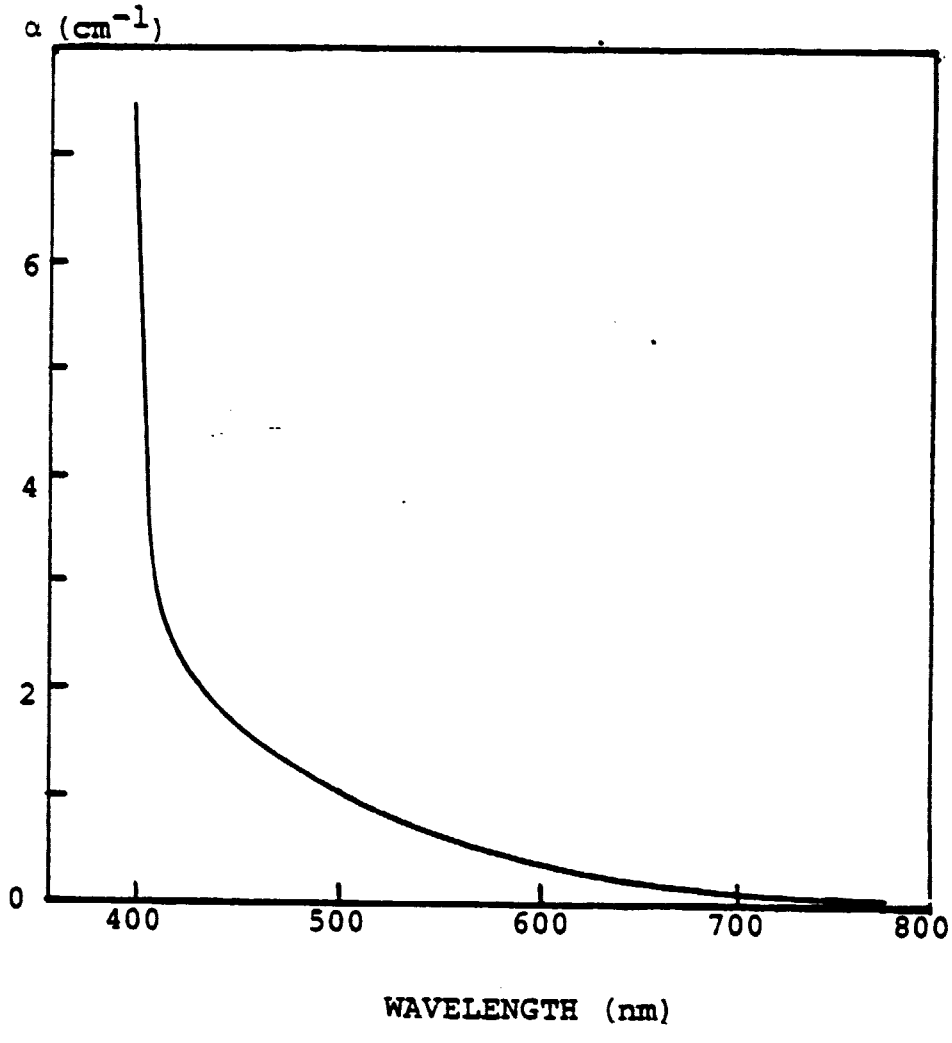

Fig. 22. Optical absorption of $BaTiO_3$ single crystal.

data were extremely erratic. Had we more time we would have tried evaporated silicon as a filler material. In what follows we describe our inconclusive results obtained with the silver paste.

Since one of our objectives was to check the additivity of the photovoltage from grain we embedded a test wire into each groove when it was filled with silver paste (Fig. 23). Before illumination, a poling voltage (200-300 V) was applied between sequential pairs of test wires in order to overcome any depolarization that might have occurred as a result of handling. The poling voltage was applied for a period of time ranging from 10-60 seconds.

During measurement the sample was electrically shielded by placing it in a grounded aluminum box that had a small opening through which the UV illumination could reach the corrugated surface. The wires attached to the sample were brought out in a shielded cable for connection, as desired, to the terminals of a Keithley 602 Electrometer.

Measurements were complicated by a number of problems. Long time constants were encountered: the order of hours after the light was turned on or off; the order of days after poling. The photovoltages were always small (rarely more than 200 mV) and the data were not reproducible. An indication of some of these difficulties is seen by comparing Figs. 24 and 25.

The first figure shows the photovoltage obtained between two adjacent test wires measured one day after poling at 250 volts. The behavior suggests a pyroelectric transient followed by a steady photo-response. However a quite different response

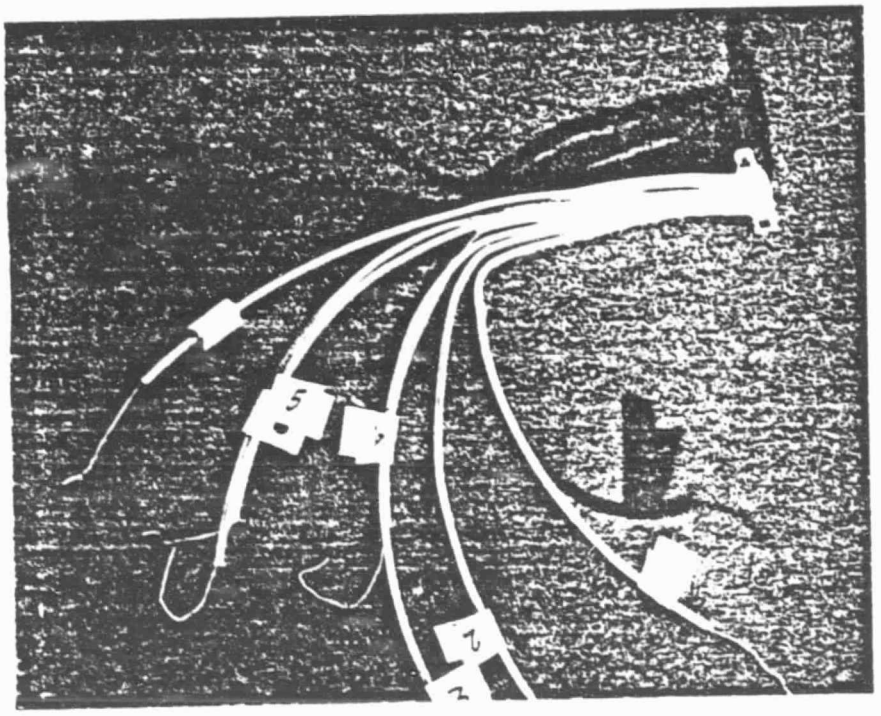

Fig. 23. Corrugated crystal with wires embedded in grain boundaries.

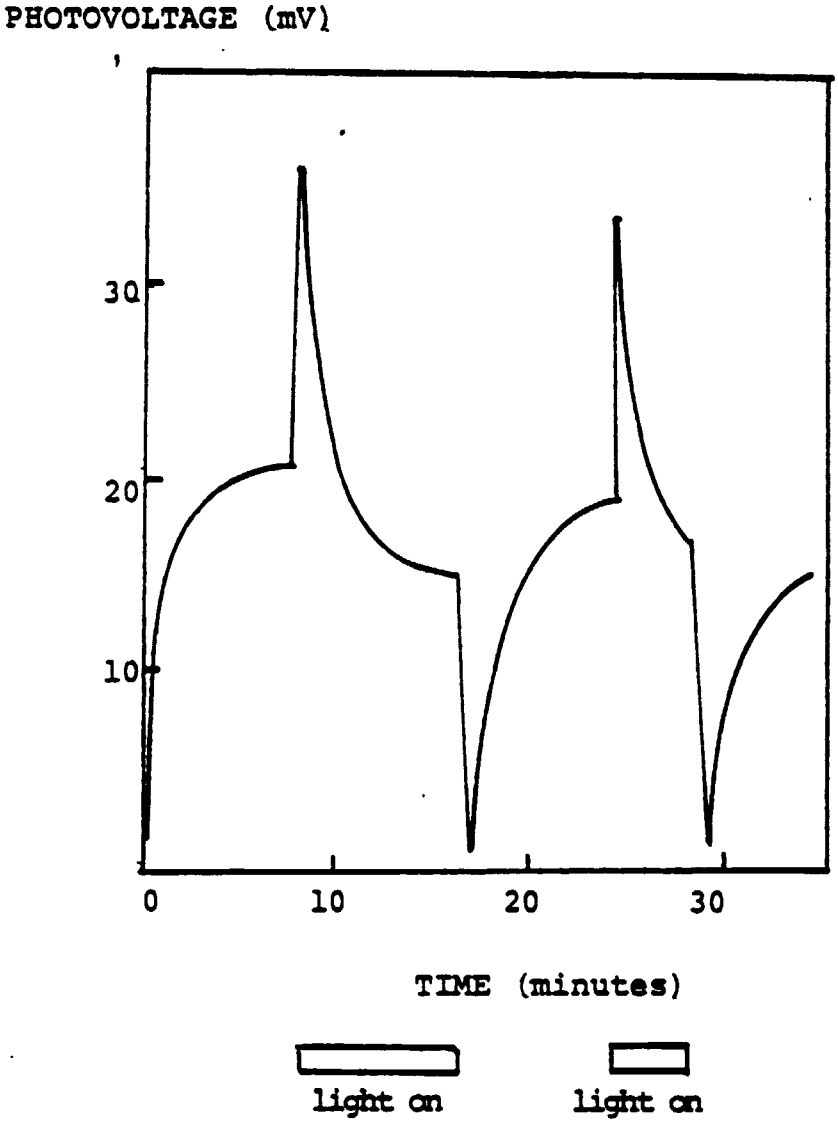

Fig. 24. Open-circuit phctovoltage measured across one segment of currugation. Measurements made one day after poling; light intensity 112 mW/cm^2.

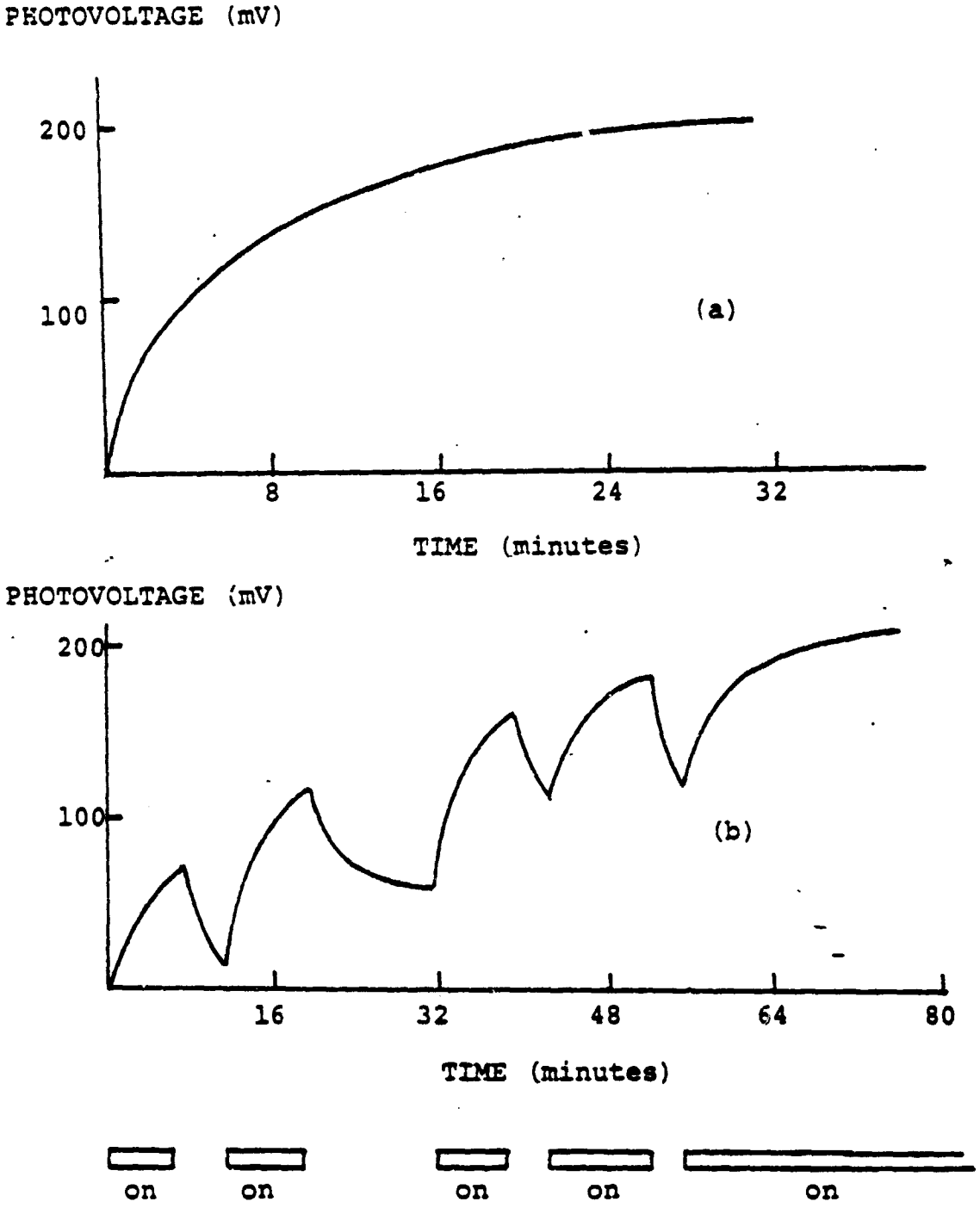

Fig. 25. Open circuit photovoltage measurements across six segments: (a) step function of light applied at t=0; (b) light turned on and off as shown. Light intensity 112 mW/cm^2.

was obtained when the sample was repoled and measured one week after poling. Here, the photovoltage approaches a final value in exponential fashion with a time constant of approximately 7 minutes. This long delay, far too long to be explained by simple dielectric relaxation time or by an RC-circuit time constant, may well be associated with relaxation processes occurring within the ferroelectric. The polarity of the photovoltage had the same sense as observed in the ceramics. The voltage between adjacent corrugation segments showed variations that were often quite large.

The photoresistance of the sample, measured as a function of light intensity, exhibited behavior similar to that seen in ceramic samples (Fig. 26).

The fact that the photovoltages were weak, erratic, and dependent on the past history of electrical treatment made it very difficult to establish an experimental procedure that we had much confidence with. The dependence of results on how the sample was allowed to "age" after poling was particularly troublesome because it meant that even a simple experiment had to stretch out over a long period of time.

V. SUMMARY AND RECOMMENDATIONS

Although the existence of anomalously large open-circuit photovoltages in ferroelectric ceramics and single crystals is a well documented experimental fact, theoretical explanations for this behavior leave much to be desired. The theories that do exist range from the qualitative to the semi-quantitative. The

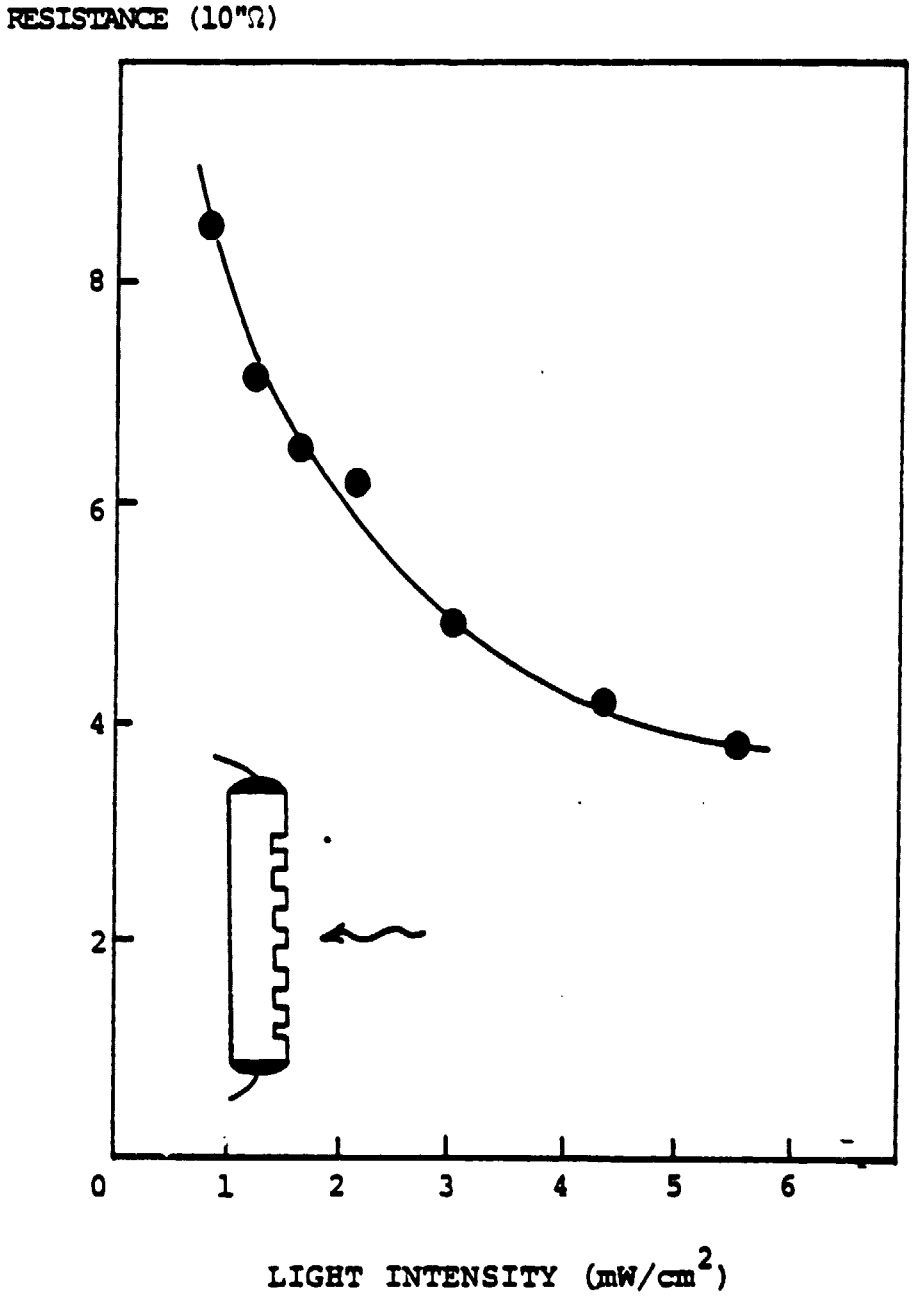

Fig. 26. Photoresistance of $BaTiO_3$ crystals as a function of light intensity. No filler material in grooves.

latter typically involve the introduction of ad hoc assumptions and arbitrarily assigned parameter values.

If there is to be any hope of providing the experimental basis for a sound theory of the anomalous effect it will be necessary to carry out studies on crystals of carefully controlled composition. In most cases, investigators have used "off-the-shelf" crystals that have been grown for general electrooptic or ferroelectric use. These materials contain incidental impurities, usually transitions metals, which appear to be responsible for the large photovoltage. In some cases, crystals with deliberately doped impurities, e.g. Fe, have been grown for study, but there has been no attempt to grow a series of crystals ranging from the extremely pure through a sequence containing increasing concentrations of controlled dopants. Such crystals are needed to establish correlation between photovoltaic effect and dopant type and concentration. (They would also be useful to obtaining a better understanding of the photorefractive effect in ferroelectrics, a subject of growing interest to researchers in the field of nonlinear optics.)[10]

It seems very likely that the photovoltaic effect in ceramics is a composite of the bulk effect found in single crystals plus effects associated with the discrete grain structure of the ceramic. What is called for, in understanding ceramics, is a program of investigation that starts with the single crystal and proceeds to add the grain boundary as the next complication. This was the approach taken in our program where we attempted to use a single crystal in a form that simulated a ceramic structure. Unfortunately, the crystal available to us did not have a

large intrinsic photovoltage, nor were we able to demonstrate the existence of any large voltages arising at our simulated grain boundaries. Perhaps the choice of silver paste as the "grain boundary" filler was the flaw in our experiments and we should have chosen other fillers, e.g. sputtered $BaTiO_3$. However, to do so would have required an effort beyond the support level provided, and we did, in fact, expect that the metal-insulator boundaries, made asymmetric by the presence of the spontaneous polarization, might behave somewhat as an additive series connection of Schottky-like photodiodes.

We have stressed the importance of proceeding from the crystal to the ceramic but we also recognize that to carry out the full single crystal program we have described would be an expensive way of attacking the ceramic problem. A more practical approach would be to begin with a program aimed at maximizing the photovoltaic effect in a ceramic. Many ceramic compositions are possible but the choice is subject to a number of constraints: the ceramic must also be available in single crystal form, if the connection between ceramic and crystal is to be made; the material should have ferroelectric properties that are well known, and should have a reasonably low coercive field so that the polarization state can be readily altered. Lithium niobate, for example, is ruled out because it does not meet the last requirement, while the more complex ferroelectrics, such as the lead zirconates/titanates, cannot be grown as large single crystals. The material of clear first preference is barium titanate. We suggest that the photoeffect in thir compound be studied as a

function of transition metal dopants (Fe, in particular) and of parameters that affect the electrical conductivity: oxidation/reduction; the addition of various donor impurities (e.g. niobium). Based on the ceramic data, a few single crystals appropriately doped and heat treated, would then provide the basis for further study of both single crystal and grain boundary effects. The latter work might be done using the corrugation scheme we have attempted, or one could take a more direct approach and sinter a number of crystals together to create grain-boundary-like interfaces.

In any future work, far greater attention should be paid to the short-circuit photocurrent, this despite the fact that it is the photovoltage that is of practical interest. The physics of the photovoltaic mechanism is contained in the photocurrent. All the theories we have described, save one, recognize this fact, and all, with, again, the one exception, are transport theories. In these, the photogenerated carriers are driven through the short-circuited sample by internal driving forces of electrochemical origin (gradients in doping or in energy gap) or by anisotropic scattering as in Glass' model. In all these models the short-circuit current is the starting point and the open-circuit voltage follows as a "circuit" consequence. The model used by Brody is distinctly different in that it attempts to derive the open-circuit photovoltage as the fundamental quantity. This difference would, by itself, not be objectionable, if it were not for the fact that this model has an intrinsic flaw that brings its entire approach into question.

REFERENCES

1. P. S. Brody and F. Crowne, J. Electronic Mat. 4, 955 (1975).

2. P. S. Brody, Appl. Phys. Lett. 38, 153 (1981).

3. P. S. Brody, U. S. Patent No. 4,236,938, December 2, 1980.

4. These results have been obtained, via a slightly different approach, by J. Tauc, "Photo and Thermoelectric Effects in Semiconductors". Pergamon Press (1962); see Ch. 3.

5. A. M. Glass, D. vonder Linde, D. H. Auston, and T. Negran, J. Electronic Mat. 4, 915 (1975).

6. M. E. Lines and A. M. Glass, "Principles and Application of Ferroelectrics and Related Materials", Oxford University Press (1977); see Sec. 12.7.

7. A. C. Chynoweth, Phys. Rev. 102, 705 (1956).

8. G. F. Neumark, Phys. Rev. 125, 838 (1962).

9. W. J. Merz, Helvetia Phys. Acta 31, 625 (1958).

10. J. Feinberg, D. Heiman, A. R. Tanguay, Jr., and R. W. Hellwarth, J. Appl. Phys. 51, 1297 (1980).

APPENDIX

Charge Compensation in Ferroelectric Crystals

When a ferroelectric crystal is poled, the polarization charges developed at its surface will attract compensating charges (e.g. from the surrounding air- or from other materials in contact with the surface) that will act to neutralize the field within the ferroelectric. In Fig. A-1 the crystal shown has been poled so that its polarization P has attained the spontaneous value P_o. The discontinuity in P at x = 0 and x = L creates surface polarization charges on the planes of discontinuity ($-P_o$ at x = 0 and $+P_o$ at x = L) which act as sources of field $E_1 = -P_o/\varepsilon$ directed opposite to the polarization. In the one-dimensional geometry being used, the electric field is totally confined to the interior of the ferroelectric so that there appears to be no mechanism for attracting compensating charges within the material available for transport to the surface by the field E_1. The absence of any external field is of course an artifact of the one dimensional geometry. For any finite ferroelectric there will be a leakage field extending into the surrounding space and this will provide the source of attraction for charges existing outside the body. If the polarization charges are truly at the surface then compensating charges will be accumulated until the field within the ferroelectric is reduced to zero. It is important to recognize, however, that zero field will not be attained unless both the polarization and compensating charges occur as coincident surface sheets.

It has been suggested that the surface of a ferroelectric crystal is not identical to the interior and, as a consequence, the polarization falls in magnitude as it approaches the surface, the transition occurring in an extremely thin layer δ (<1μm). Such a layer may be the result of surface damage caused by sawing, cutting or etching, or by any process that leads to compositional or structural change at the surface. For simplicity we assume that the polarization falls linearly to zero in the transition thickness δ , in which case (Fig. A-2)

$$\begin{aligned} P &= P_o\,(x/\delta) && \text{in region I} \\ P &= P_o && \text{in region II} \\ P &= P_o\,(L-x)/\delta && \text{in region III} \end{aligned} \qquad \text{(A-1)}$$

The resultant polarization charges are determined by the relation

$$\rho_p = -\nabla\cdot\bar{P} \qquad \text{(A-2a)}$$

from which we find that ρ_p in regions I, II and III is respectively $-P_o/\delta$, 0, $+P_o/\delta$ (Fig. A-3).

From the charge distribution we obtain the electric field E_1 by integration:

$$E_1 = \frac{1}{\epsilon}\int_{x=0}^{L} \rho_p\, dx \qquad \text{(A-2b)}$$

where we must use the boundary condition $E_1 = 0$ at $x = 0$. The resultant field (Fig. A - 4) varies linearly in the regions I and III and has its previous, constant value $E_1 = -P_o/\varepsilon$ in region II.

We now consider the effect of external compensating charges occurring at the surfaces $x = 0$ and L. These charges wiil, as we have noted, be attracted to the surface by the leakage field that occurs when the ferroelectric is a finite body. However, we can stay within the framework of the one dimensional problem by recognizing that the driving force for compensation is the attempt of the system to reduce its free energy to a minimum. We shall, therefore, proceed by assuming that the sheets of compensating charge at $x = 0, L$ do not have the magnitude P_o but instead have a value αP_o where α is a constant to be determined from the requirement that the free energy be a minimum.

We, first, note that the field produced by the two sheets of compensating charge is $E_2 = \alpha P_o/\varepsilon$. The resultant field E is equal to $E_1 + E_2$. Thus, in region I

$$E_I = -(P_o/\varepsilon)\ (x/\delta) + \alpha(P_o/\varepsilon) \qquad (A\text{-}3)$$

while in region II

$$E_{II} = (1-\alpha)\ (P_o/\varepsilon) \qquad (A\text{-}4)$$

The free energy of the system is given by

$$u = \frac{1}{2}\,\varepsilon \int_0^{\delta} E_I^{\,2}\, dx + \frac{1}{2}\,\varepsilon \int_{\delta}^{L-\delta} E_{II}^2\, dx + \frac{1}{2}\,\varepsilon \int_{L-\delta}^{L} E_{III}^2\, dx \qquad (A\text{-}5)$$

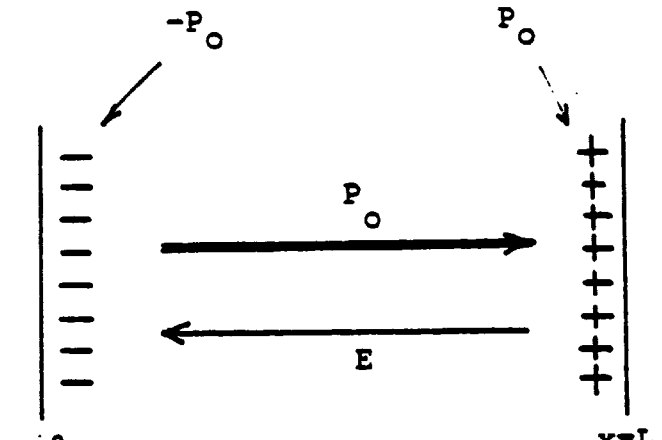

Fig. A-1. Fields and charges in compensated polarized crystal. Polarization charges are per unit area.

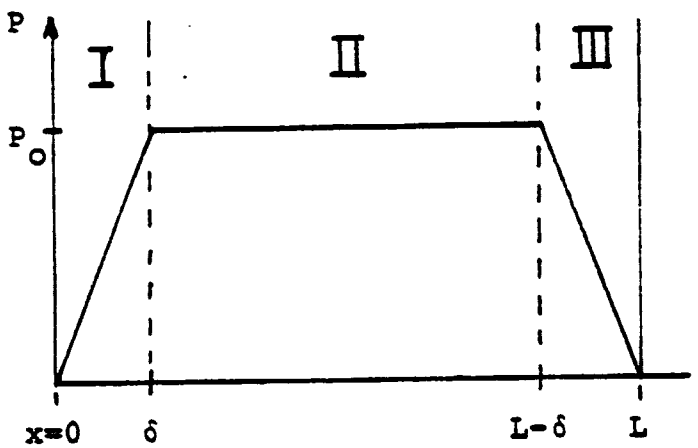

Fig. A-2. The polarization is assumed to fall linearly to zero in a surface "skin" of thickness δ.

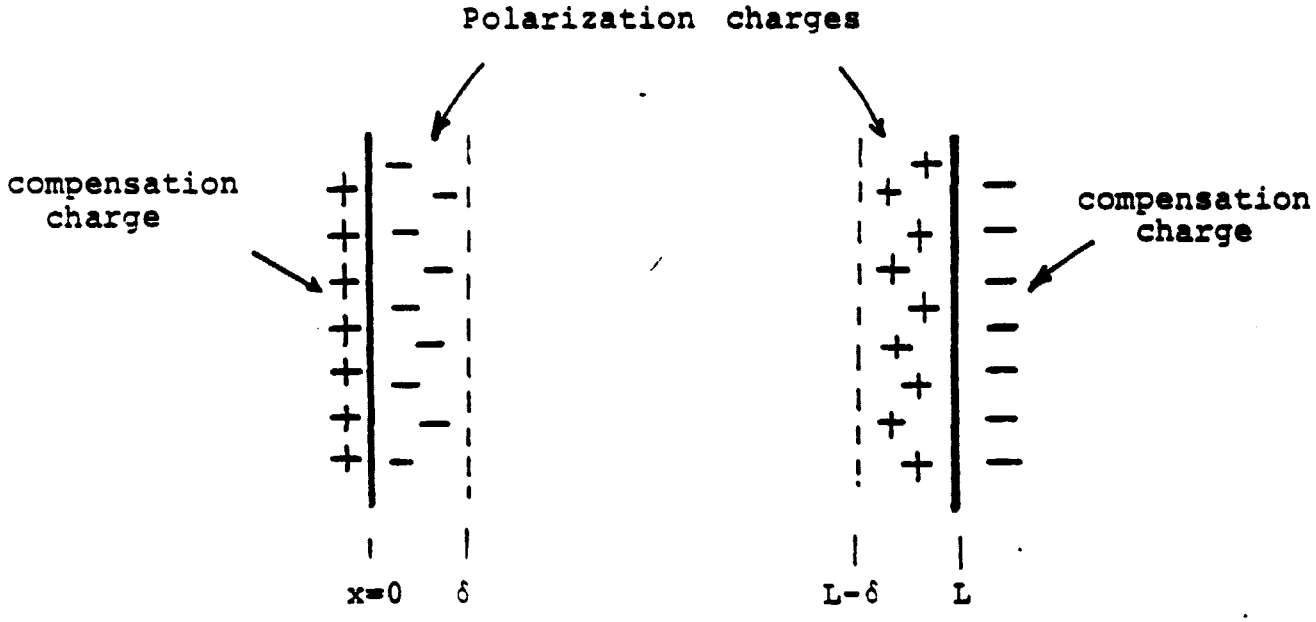

Fig. A-3. Polarized crystal of Fig. A-2 with surface compensation charges.

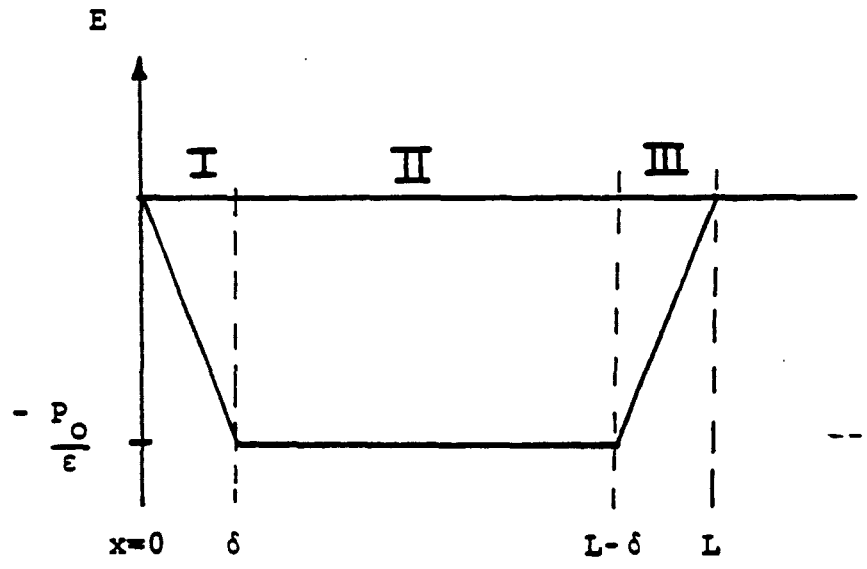

Fig. A-4. Field produced by polarization charges acting alone.

where the first and third terms are obviously equal. The resultant free energy is

$$U = \frac{P_o^2}{2\varepsilon}\left[\frac{2}{3}(3\alpha^2-3\alpha+1)\,\delta + (1-\alpha)^2\,(L-2\delta)\right] \qquad (A-6)$$

Employing the condition for minimum free energy, $dU/d\alpha = 0$, we find

$$\alpha = 1 - \frac{\delta}{L} \qquad (A-7)$$

and it follows that

$$E_I = (P_o/\varepsilon)\left(1 - \frac{\delta}{L} - \frac{x}{\delta}\right) \qquad (A-8)$$

$$E_{II} = -(P_o/\varepsilon)\,(\delta/L) \qquad (A-9)$$

Note that the field in the transition layer attains its maximum value

$$E_{Imax} = (P_o/\varepsilon)\left(1 - \frac{\delta}{L}\right) \qquad (A-10)$$

at the surface, and that in the bulk there is incomplete compensation (Fig. A-5). When the thickness of the transition layer goes to zero the compensation becomes perfect, i.e. $\alpha \to 1$ and $E_{II} \to 0$.

The potential difference between $x = 0$ and $x = L$ is found by integrating the field, i.e.

$$V = -\int_0^{\delta} E_I\,dx - \int_{\delta}^{L-\delta} E_{II}\,dx - \int_{L-\delta}^{L} E_{III}\,dx \qquad (A-11)$$

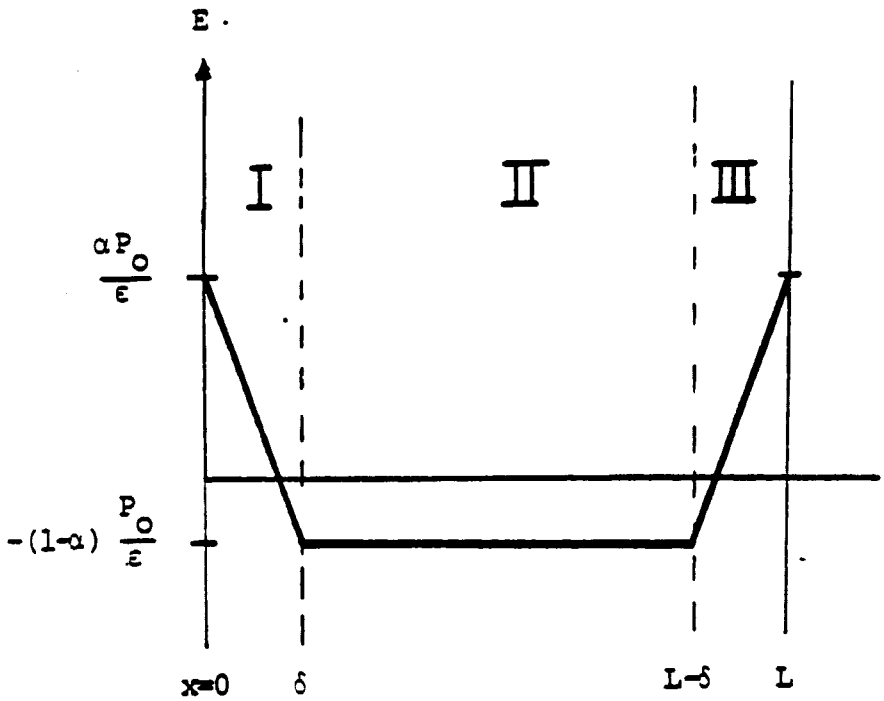

Fig. A-5. Field distribution for state of minimum free energy.

The result of this integration is V = 0. Thus, the requirement for equilibrium that the system be in a state of minimum free energy implies that the potential across the compensated ferroelectric be zero.

The configuration of polarization and compensation charges we have just considered slightly different from the one employed by Brody in analyzing the photovoltaic effect in a ferroelectric ceramic. Brody assumes that the spontaneous polarization terminates abruptly as shown in Fig. 9 and that the compensation charges are distributed uniformly over a skin of thickness δ. The field produced by this charge distribution is shown in Fig. 10. The parameter α may be found, as above, by minimizing the free energy or, as Brody has done, by setting the potential drop across the charge system equal to zero. The result is

$$\alpha = \frac{L-2\delta}{L-\delta} \qquad \text{(A-12)}$$

with $\delta \ll L$, we obtain

$$\alpha = 1 - \frac{\delta}{L} \qquad \text{(A-13)}$$

the same value found for the compensation/polarization charge configuration in Fig. A-3.